Zhao *et al. Biochar* (2025) 7:77
https://doi.org/10.1007/s42773-025-00467-x

Biochar

REVIEW

Open Access

Unlocking the potential of element-doped biochar: from tailored synthesis to multifunctional applications in environment and energy

Junqi Zhao[1], Yunqiu Jiang[2], Xinyu Chen[1], Chongqing Wang[1] and Hongyan Nan[1*]

Abstract

Biochar, a versatile environmental material, has gained significant attention for its exceptional physical and chemical properties. This comprehensive review explores the innovative preparation methods of element-doped biochar, highlighting their enhanced functionalities and groundbreaking applications across diverse fields. Drawing from conventional approaches, this study systematically investigates in-situ and exogenous doping techniques, examining their distinct advantages, limitations, and profound impacts on the morphological structure and surface chemistry of biochar. By integrating multiple elements, the research reveals how doping significantly improves the adsorption capacity, catalytic efficiency, and electrochemical performance of biochar, offering opportunities for its potential use in environmental remediation, soil enhancement, energy conversion, and even cosmetic applications. Moreover, this study introduces an original framework of "preparation–structure–performance–application", emphasizing the importance of optimizing doping strategies and element selection to maximize versatility of biochar across multiple domains. Beyond basic insights into existing knowledge, this review provides novel perspectives for future research, particularly in areas such as carbon sequestration, pollutant adsorption, and advanced catalysis. This comprehensive synthesis not only synthesizes existing knowledge but also delivers fresh, innovative insights into the untapped potential of element-doped biochar, propelling transformative progress in sustainable materials science and beyond.

Highlights

- Element doping strategies unlock potential of biochar in environment and energy storage.
- Comparing the pros/cons about in-situ/exogenous synthesis pathways of element-doped biochar.
- Decoding the relationship between structure-performance and applications of element-doped biochar.
- Proposing a systematical "synthesis–performance–application" paradigm of element-doped biochar.

Keywords Biochar, Element doping, Soil improvement, Supercapacitor, Pollutant removal

*Correspondence:
Hongyan Nan
nanhongyan@zzu.edu.cn
Full list of author information is available at the end of the article

Graphical Abstract

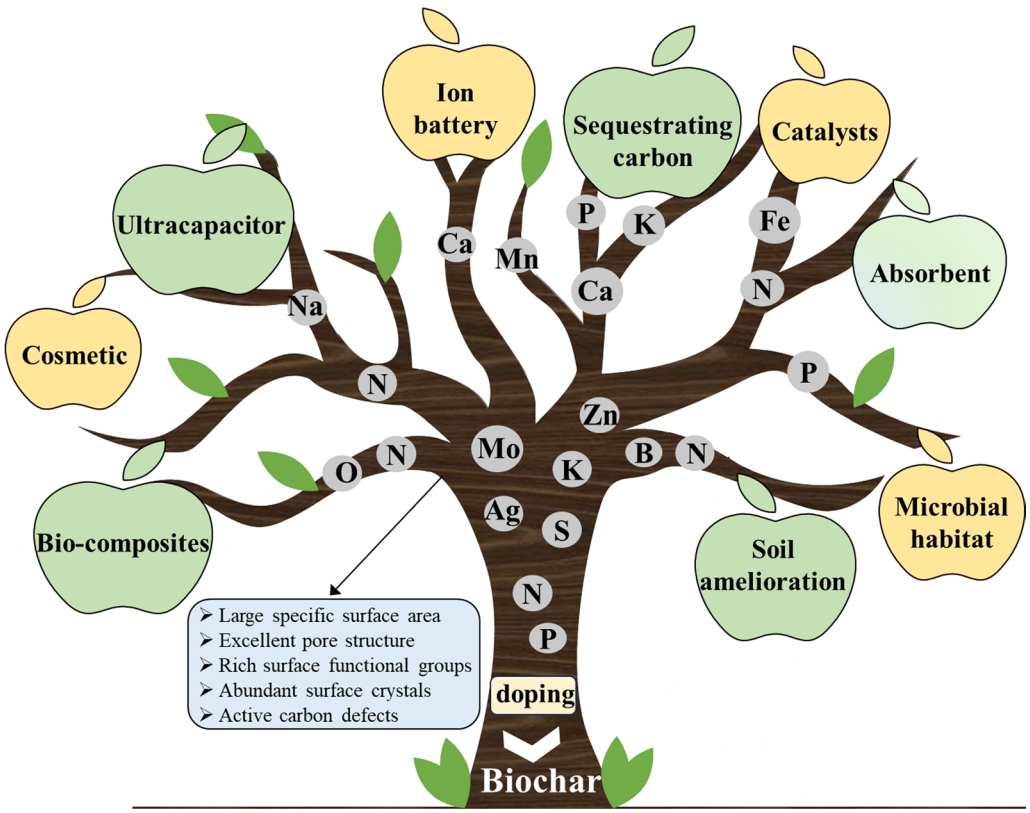

1 Introduction

Advanced carbon materials such as graphene, activated carbon, and carbon nanotubes (CNTs) have been widely utilized across diverse industries including the chemical industry, electronics, and aerospace. These materials are distinguished by their large specific surface area, customizable pores, high electrical conductivity, diverse precursors, and strong mechanical properties (Li et al. 2021a; Pamphile et al. 2023; Shu et al. 2023; Wang et al. 2020). For instance, a novel graphene skinned fiber material has demonstrated remarkable advantages in aircraft anticing and icing applications, despite the notable drawback of high production costs (Qi et al. 2024). In addition to graphene, carbon nanotubes represent another significant carbon material characterized by their one-dimensional structure. Extensive research over the past two decades in the electrical and electronics domains has yielded extensive findings on carbon nanotubes, which exhibit distinctive morphology and exceptional electrochemical properties, offering promising prospects for energy storage applications. Furthermore, carbon nanotubes have been successfully integrated as active materials and carriers within battery and supercapacitor electrodes (Sun et al. 2017). However, despite their advanced structural preparation methods, expensive synthesis procedures, and poor dispersibility, the practical application of carbon nanotubes remains limited (Lavine 2018). Consequently, there is a pressing need to develop cost-effective, efficient, and readily available materials to expand the application scope of carbon materials (Alhashimi & Aktas 2017).

Biochar, a carbon-rich material derived from the pyrolysis of biowaste, has attracted significant attention from researchers in recent years (Aller 2016; Chen et al. 2019;. Gao et al. 2023a; Lin et al. 2023a, b; Zhou et al. 2022a, b). Initially recognized as a soil amendment for improving soil fertility and enhancing carbon sequestration through soil application (Aller 2016; Moralı et al. 2016), advancements in biochar functionalization have expanded its applications into diverse fields such as energy conversion and storage, pollutant treatment, and environmental remediation (Fig. 1) (Resego et al. 2023). Functionalization aims to improve the physical and chemical properties of biochar, including surface area, porosity, chemical

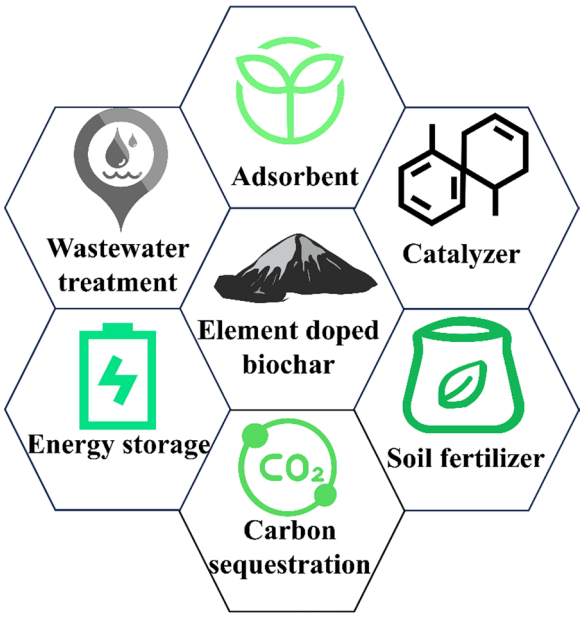

Fig. 1 Application areas of elementally doped biochar

functional groups, and thermal stability, as well as its electrochemical properties, such as conductivity, redox activity, and electrochemical stability. Additionally, it improves the availability of surface active sites, including Bronsted acid sites, Lewis acid sites, base sites, and redox sites (Deng et al. 2022; Li et al. 2017a, b; Tan et al. 2020). Current methods for preparing functional biochar include ball milling, template methods, chemical activation, and elemental doping (Li et al. 2017a, b; Song et al. 2021; Wu et al. 2022).

Among these, element doping has emerged as a simple yet effective strategy for functionalizing biochar, offering significant improvements in its structure and properties. Although not as extensively studied as other modification techniques, element doping has demonstrated remarkable potential in enhancing biochar materials (Wan et al. 2020; Wang et al. 2023a, 2018). Researchers have successfully doped various biowastes with elements, revealing that the incorporation of suitable elements can enhance the mechanical, thermal, and chemical stability of biochar, along with other desirable properties. This has broadened its applications in energy storage, environmental remediation, and beyond (Tang et al. 2021). For instance, biochar doped with nutrient elements such as potassium (K), nitrogen (N), and phosphorus (P) has shown promise as an innovative soil amendment, improving soil fertility, promoting plant growth, and ultimately increasing crop yield and quality (Anum et al. 2024; Liu et al. 2024; Xin al., 2021). In the energy sector, biochar doped with elements like nitrogen (N) and sulfur (S) has demonstrated potential as a novel energy storage material, leveraging synergistic effects between different elements to advance research in this field (Kong et al. 2023; Wan et al. 2020).

The practice of element doping offers numerous advantages to biochar, driving researchers to further explore this area to optimize its utilization across various fields. Current studies primarily focus on single-element doping and its applications, highlighting the potential of doped biochar in environmental, catalytic, and energy-related applications (Table 1). This study aims to provide a systematic and comprehensive review of element-doped biochar, focusing on its preparation methods, structural properties, enhanced functionalities, and diverse applications. Unlike previous reviews, we introduce an original "preparation–structure–performance–application" framework to guide the optimization of doping strategies and element selection for targeted applications. By exploring innovative in-situ and exogenous doping techniques, we uncover their unique advantages and limitations, while investigating the transformative impact of doping on biochar morphology, structure, and surface chemistry. Furthermore, we identify emerging and unconventional applications of element-doped biochar, such as in cosmetics and advanced catalysis, which expand its potential beyond traditional uses. This review not only consolidates current knowledge but also provides innovative insights into the untapped potential of element-doped biochar, paving the way for transformative advancements in sustainable materials science.

2 Element doping mode

2.1 In situ *doping*

In situ doping, also known as self-doping, involves the direct carbonization of biowaste containing the desired element to produce biochar (Fig. 2). This method facilitates the incorporation of heteroatoms into the biochar matrix, altering its performance such as specific surface area, functional groups, surface crystals, carbon defect, and active site (Zheng et al. 2023). Common plant-based biowastes, including bamboo, rice husks, honeysuckle, and catkins, primarily consist of carbon (C) and oxygen (O), with trace amounts of nitrogen (N), phosphorus (P), and sulfur (S). Table S1 summarizes the elemental composition (C, N, O, P, S) of various plant-based biowastes based on a comprehensive literature review. Through simple pyrolysis, hydrothermal, or microwave processing, elements like N, O, P, and S can undergo self-doping in biochar. For instance, the inherent N and O in bamboo can be doped into biochar, promoting the formation of porous structure (Chaturvedi et al. 2023). Similarly, Chen et al. (2023) reported that pyrolyzing fish scales, which are rich in N, S, and O, resulted in biochar with enriched

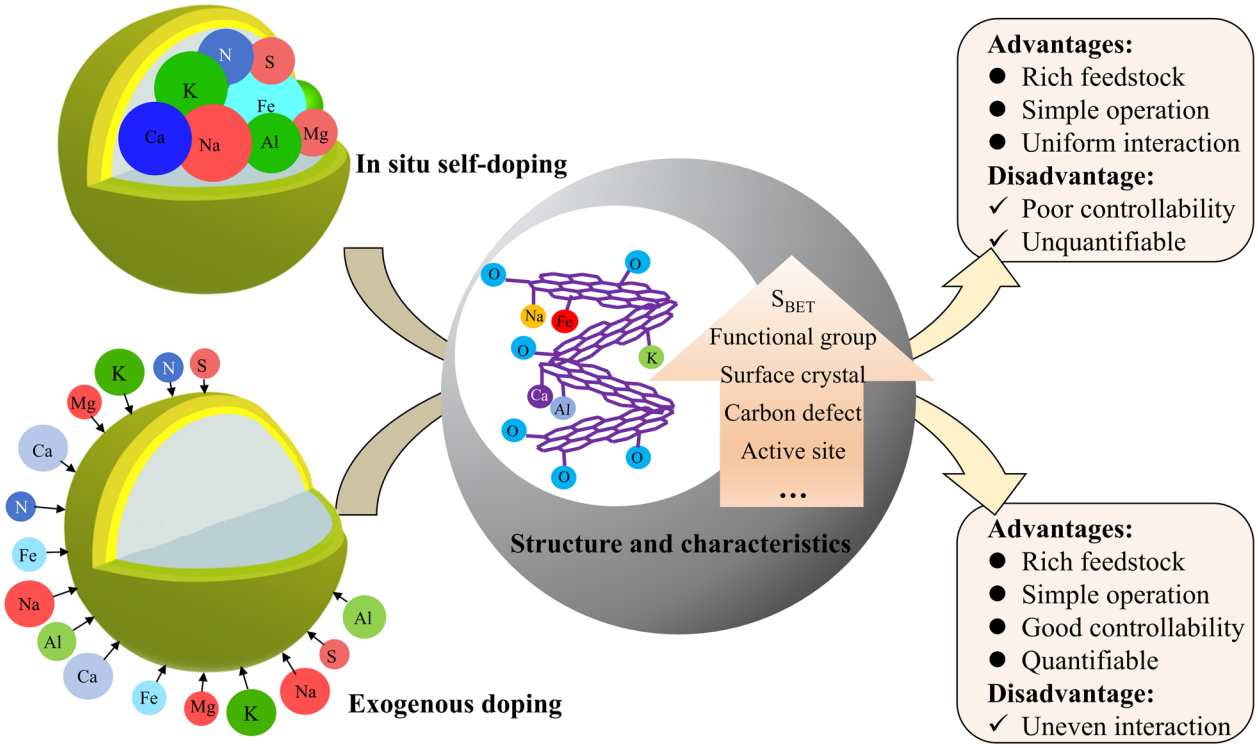

Fig. 2 The distinction between in-situ and exogenous doping

elemental contents of 65.59% N, 3.41% S and 0.17% O. While self-doping is straightforward and cost-effective, accurately quantifying the type, content, and composition of elements in precursor materials remains challenging. This variability complicates the reproducibility and standardization of research outcomes (Fig. 2).

2.2 Exogenous doping

Certain biowastes, such as bagasse, corn stalks, fruit hulls, grapefruit peels, and banyan trees, have low heteroatom content and require the introduction of exogenous dopants for element doping, a process known as exogenous doping. Compared to in-situ doping, exogenous doping offers better control and easier quantification of dopant levels (Fig. 2). Exogenous doping techniques are broadly categorized into chemical vapor deposition (CVD) and direct contact methods (Table S2) (Ahmad et al. 2023). The CVD method allows for the precise deposition of dopants onto biochar surfaces through gas-phase reactions, and it offers excellent control over doping uniformity and concentration (Table S2). For instance, Chen et al. (2020) successfully obtained N-doped biochar by pyrolyzing bamboo in an ammonia atmosphere. However, the utilization rate of this straightforward CVD method is not high and it is energy-intensive and expensive, limiting its use to high-value applications (Liao et al. 2024). In contrast, the direct contact methods, such as wet impregnation and dry mixing, are more versatile and cost-effective (Table S2). These methods involve mixing biowaste with dopant-containing materials followed by pyrolysis (Anum et al. 2024; Ding et al. 2020). For instance, Wan et al. (2022) prepared S-doped biochar by pyrolyzing biowaste mixed with S_8 precipitates, while Sun et al. (2023a) produced N-doped biochar by ball milling the corn stalk biochar impregnated with urea. Table S2 compares the respective advantages, limitations, and suitability of wet impregnation and pyrolysis with precursors. Wet impregnation involves immersing biochar in a dopant solution, followed by drying and thermal treatment. It is cost-effective and scalable, making it suitable for large-scale applications (Li et al. 2021a, b; Verdida et al. 2023). However, it requires careful control of solution concentration and immersion time to ensure uniform doping. Co-pyrolysis with precursors is another effective method, where biomass is pyrolyzed alongside dopant-containing materials. This technique is simple and achieves homogeneous doping, but the choice of precursors and pyrolysis conditions significantly influences the final properties of the doped biochar (Li et al. 2023b; Zang at al. 2022a)

To achieve optimal results in the elemental doping of biochar, it is crucial to follow best practices tailored to the desired properties and applications. In-situ doping is ideal for uniform doping during biomass pyrolysis, using biomass naturally rich in the desired element or pre-treated with dopant precursors, though it imposes strict requirements on raw materials. Exogenous doping, on the other hand, offers flexibility and precision. For instance, wet impregnation is a cost-effective and scalable method, achieving uniform dopant distribution by optimizing solution concentration and immersion time. Meanwhile, CVD enables high-precision doping through controlled gas-phase reactions, ensuring uniform dopant deposition. Selecting the appropriate biowaste, doping method, and dopant content based on the intended application is essential for advancing the development and application of elementally doped biochar.

3 Types of doping elements

3.1 Nitrogen doping

Nitrogen (N) is a widely used element for doping biochar, significantly enhancing its functional properties. N-rich biowastes, such as algae, microorganisms, and animal dung, naturally contain high nitrogen levels, enabling the direct preparation of N-doped biochar through self-doping (Feng et al. 2024a). For low-nitrogen feedstocks, external nitrogen sources like NH_3, urea, and ammonium salt are introduced (Wan et al. 2020). N doping catalyzes ester hydrolysis reactions, with surface basic functional groups acting as alkali catalysts that promote nucleophilic addition reactions with carbonyl groups, breaking ester bonds (Chen et al. 2020). N in doped biochar typically exists in five forms: amination functional groups, pyridine N (six-membered heterocyclic rings), pyrrole N (five-membered heterocyclic rings), graphite N (sp^2-hybridized nitrogen adjacent to three sp^2-hybridized carbons), and nitrogen oxides ($-NO_x$) (Fig. 3a, b and Table S3) (Gopalakrishnan & Badhulika 2020). Pyridine-N and pyrrole-N are located at edge or defect sites, while graphite-N replaces carbon atoms within the graphite layer, introducing additional π electrons. These nitrogen configurations coexist in biochar, with their relative concentrations adjustable based on the doping level (Wang & Wang 2019). N doping primarily enhances the pore structure, specific surface area, catalytic activity, adsorption capacity, energy storage capability, and electrical conductivity of biochar, without significantly altering its fundamental structure (Yu et al. 2022). Table S3 summarizes the types of N species and their application in N-doped biochar. For example, Ling et al. (2017) used

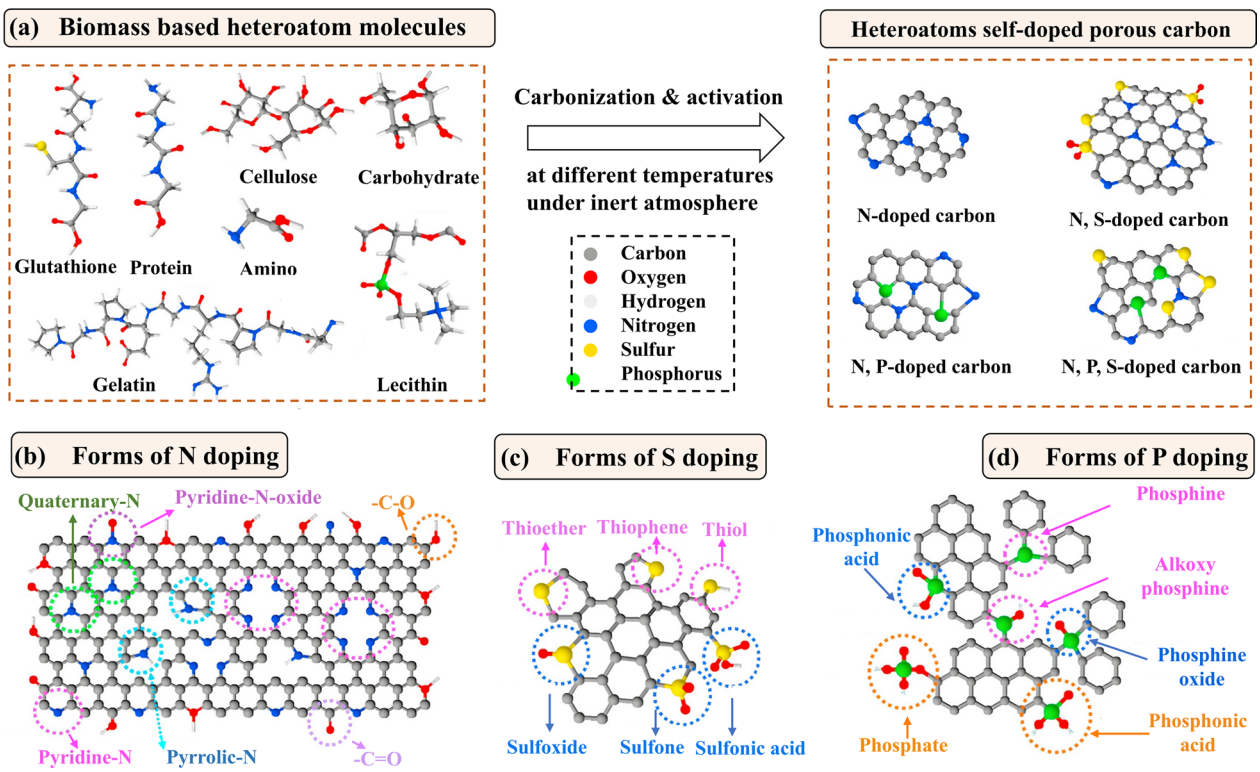

Fig. 3 The morphologies of N, P and S in biomass, as well as the main forms of N, P and S doping in biochar. Adapted from Gopalakrishnan & Badhulika (2020)

N-rich hydrophytes to produce biochar enriched in pyrrole-N and pyridine-N, which adsorbed Pb(II) through surface coordination. Mian et al. (2019) pyrolyzed agar in an ammonia atmosphere to generate biochar with high pyridine-N and graphite-N content, demonstrating excellent catalytic degradation of organic pollutants. Yuan et al. (2022) synthesized N-doped biochar from reed and chlorella, achieving superior capacitance for energy storage. Additionally, N-doped biochar serves as an effective catalyst carrier, enhancing the dispersion and stability of loaded metals or metal oxides (Chen et al. 2019; Sun et al. 2023b, c, d; Zaman et al. 2024).

3.2 Oxygen doping

Oxygen (O) is a widely used dopant in biochar due to its high electronegativity, which significantly influences electron distribution. O-doped carbon materials often exhibit redox-active functional groups on their surface, such as –COOH, –OH, and C=O. These groups act as electron donors, promoting the generation of free radicals for oxidation reaction (Wang et al. 2022). For example, Wang et al. (2022) produced O-rich biochar by pyrolyzing sawdust with magnesium carbonate pentahydrate at 800 °C. They observed a significant increase O-containing functional groups (–COOH, OH, and C=O), particularly C=O, which increased by 16.17% compared to untreated biochar. The C=O group plays a dual role: facilitating electron transfer and serving as an adsorption site for immobilizing pollutants (Chacón et al. 2020). Dinh et al. (2022) demonstrated that O-containing functional groups in O-doped biochar degrade sulfadiazine by cleaving S–N bonds and heterocycles while oxidizing amino groups. During pyrolysis, the introduced O combines with C and N to from volatile compounds, creating defects and smaller pores on the biochar surface. This enhances specific surface area and pore volume. However, at high pyrolysis temperatures, carbon structures accumulate, reducing these defects (Zhang et al. 2022b).

3.3 Sulfur doping

Sulfur (S) is a widely used dopant in biochar due to its eco-friendly nature and minimal secondary pollution. Naturally present in most biomass feedstocks, S doping offers favorable conditions for tailoring structural and functional properties of biochar (Zhang et al. 2023b). The introduction of S alters the internal structure of biochar, often reducing pore size as S atoms replace O-containing groups on the surface, leading to pore blockage (Wu et al. 2018). This structural modification enhances the catalytic ability of biochar (Ding et al. 2020). Additionally, although S and C belong to the same main group and share similar electronegativities ($\chi_S = 2.58$, $\chi_C = 2.55$), the larger atomic size of S creates voids within the carbon structure during pyrolysis. This increases the distance between carbon layers, generates porous defects, and enhances porosity and specific surface area (Ding et al. 2020).

S in doped biochar typically exists in two forms: thiophene-S (–C–S–C) and oxidized-S [$C–SO_x–C$, where x=2, 3, 4] (Figure 3a and c) (Hassaan et al. 2024; Oh et al. 2021). The content of thiophene-S generally increases with higher S doping rates, while oxidized-S decreases (Guo et al. 2020a; b). These S configurations provide additional active sites and elongate the C–C bond length in sp^2-hybrid carbon, facilitating electron transfer. As a result, S-doped biochar has been extensively studied for pollutant adsorption. For example, Yang et al. (2022a; b) prepared S-doped corn stalk biochar via ball milling, achieving a maximum tetracycline adsorption capacity of 505.68 mg g^{-1}. However, excessive S doping can negatively impact the performance of biochar. Guo et al. (2020a; b) reported that high S levels can collapse pore structures, reducing the exposure of active sites. Ding et al. (2020) also noted that S doping can impair the catalytic performance of rice straw biochar due to the formation of spin charges in the carbon lattice, attributed to the similar electrochemical properties of S and C. These findings highlight the need for further research to optimize S doping levels and understand the specific interactions between sulfur and the carbon structure of biochar. By balancing S incorporation, researchers can maximize the benefits of S-doped biochar while mitigating potential drawbacks.

3.4 Phosphorus doping

Phosphorus (P) is a widely used dopant in biochar, with applications spanning adsorption and energy storage. The larger atomic size of P (100 pm) compared to C (70 pm), combined with its variable valence states and electron-donating capability, enables P atoms to dope prominently outside the graphene plane. This results in local structural deformations in the hexagonal carbon framework, avoiding steric hindrance commonly observed in planar N-doped carbon materials (Huang et al. 2023a; b). The difference in covalent radii between P and C allows for the regulation of local electron distribution and the creation of structural defects within the carbon lattice. These defects generate additional active sites, optimizing the electronic structure and surface charge distribution of biochar (Patel et al. 2016; Song et al. 2020). During pyrolysis, the introduction of P-containing substances often incorporates oxygen, forming C–O–P and C–P–O bonds (Wang et al. 2023a). Wu & Radovic (2006) observed that as pyrolysis temperature increases, the P–O bond in C–O–P breaks, releasing CO and leaving positively

charged P atoms. These P atoms then participate in electrophilic addition reactions with unsaturated carbon structures, forming C–P–O bonds. Higher concentrations of C–O–P and C–P–O bonds enhance the specific surface area and adsorption capacity of biochar, with C–O–P bonds also protecting C atoms during pyrolysis (Yang et al. 2024a; b). P in doped biochar exists in various forms, including $-P_2O_7$, $-PO_3$, and P=O (Fig. 3d), which influence surface charge distribution and enhance adsorption by generating more negative potentials (Formula 1 – 4). However, increasing carbonization temperature reduces these functional groups, creating additional defect sites and lowering graphitization levels (Wei et al. 2023). The active components in P-doped biochar, such as C–P=O, C=O, and O–C=O groups, make it a promising alternative to commercial activated carbon. For instance, Zhou et al. (2022b) reported that P-doped biochar exhibits an adsorption capacity over 400 times higher than untreated biochar under simulated flue-gas conditions, surpassing even commercial brominated activated carbon. Moreover, using low- and medium-grade phosphate rock as a P source for doping not only supports sustainable phosphorus cycling but also contributes to environmental sustainability.

$$2H_2PO_4^- \rightarrow HPO_4^{2-} + H_3PO_4 \quad (1)$$

$$2H_2PO_4^- \rightarrow PO_3^- + H_2O \quad (2)$$

$$2HPO_4^{2-} \rightarrow P_2O_7^{4-} + H_2O \quad (3)$$

$$H_3PO_4 \rightarrow PO_3^- + H_2O \quad (4)$$

3.5 Halogen doping

Halogen elements (F, Cl, Br, I) have been explored for doping into carbon materials, including biochar and activated carbon, to modify their electronic structure, energy levels, and optical and catalytic properties (Fu et al. 2023a; Luo et al. 2022). The incorporation of halogen atoms forms C–X bonds (X=F, Cl, Br, I), leveraging the unique reactivity of halogens to tailor the electronic properties of carbon materials. For example, Fu et al. (2023a) demonstrated that the halogen doping broadens the energy levels associated with electron transitions, reduces the gap between the highest occupied molecular orbital and the lowest unoccupied molecular orbital, and significantly enhances the optical and catalytic performance of carbon materials. Similarly, Wang et al. (2021a; b) reported that halogen doping reduces the band gap, increases the generation of photoinduced charge carriers, lowers electron transfer resistance, and improves the photocatalytic activity of halogen-doped biochar. Despite these advantages, research on halogen-doped biochar remains limited due to the toxicity of many halogen sources, such as fluorine and chlorine compounds (Yuan et al. 2023a, b). This toxicity complicates the accurate determination of the position and quantity of doped halogen atoms. Additionally, the high reactivity of halogens poses challenges in controlling the doping process. To address these issues, future efforts should focus on identifying environmentally friendly halogen sources to replace toxic fluorine and chlorine compounds, as well as developing precise methods to measure halogen levels.

3.6 Metal element doping

In contrast to non-metallic elements, the doping of metal elements into biochar can cause significant alterations in its structural properties due to the reactive nature of metals. On the one hand, metal element doping promotes electron transfer rates by forming highly active substances on the biochar surface (Guo et al. 2023). For example, Fe-doped biochar exhibits excellent Fenton-like catalytic degradation performance across a wide pH range, thanks to well-dispersed Fe species, including Fe^0, Fe^{2+} and Fe^{3+} (Wang et al. 2021a, b). Liu et al. (2019) demonstrated that Fe salts undergo a sequential transformation during pyrolysis, converting into oxides (Fe_2O_3, Fe_3O_4), carbides (Fe_3C), and eventually metallic Fe (Fe^0) at elevated temperatures ($Fe^{3+} \rightarrow Fe_2O_3 \rightarrow Fe_3O_4 \rightarrow Fe_3C \rightarrow \alpha$-Fe). Similarly, Cu-doped biochar forms new Cu–O bonds and exhibits strong π-π interactions between the graphite layer and aromatic ring structure via strong hydrogen bonds, enhancing its pollutant removal efficiency (Shao et al. 2021). On the other hand, the inclusion of metal ions leads to the development of metal nanoparticles and oxides on the biochar surface. These structures act as physical barriers, protecting the biochar from oxidation and improving its stability (Yu et al. 2021a, b). For instance, Nan et al. (2020) examined the influence of alkali metals (K, Ca, Na, Mg)-doping cow dung biochar on carbon fixation capability and stability. Their study demonstrated that alkali metal oxides formed during pyrolysis act as dual-functional agents: (1) physical barriers restricting the volatilization of carbon-containing compounds and (2) CO_2 adsorbents, thereby enhancing carbon retention. In contrast, Yu et al. (2021a; b) discovered that metal nanoparticles and oxide coatings on biochar surfaces could paradoxically accelerate carbon decomposition. This catalytic effect destabilized the carbon skeleton, leading to pore collapse and reduced specific surface area (SSA) and porosity, particularly under rapid microwave pyrolysis conditions. The apparent contradiction between these findings can be rationalized through pyrolysis method and the type of metal and

biowaste. From the perspective of pyrolysis method, Nan et al. (2020) employed conventional tube furnace pyrolysis with slower heating rates (5–10 °C min^{-1}), whereas Yu et al. (2021a; b) utilized microwave-assisted pyrolysis achieving ultra-fast heating (> 100 °C s^{-1}). The latter method promotes intensive metal–biomass interactions through localized plasma formation. Considering the metal type, free alkaline earth ions (Ca^{2+}, Mg^{2+}) in Nan's study exhibited pore-expanding effects via gas evolution reactions, while Yu's solid mineral precursors (e.g., bentonite) generated dense oxide layers that obstructed pore networks. From the perspective of biowaste, high-ash cow dung in Nan's work provided intrinsic mineral templates for pore development, contrasting with the low-ash lignocellulosic biomass in Yu's study where exogenous minerals dominated structural evolution. These mechanistic insights reveal that metal dopants predominantly catalyze carbon skeleton reorganization rather than simple decomposition. The net outcome depends on the interplay between metal mobility, heating dynamics, and biomass matrix effects. Future research should employ advanced characterization techniques to resolve real-time structural transformations and establish predictive models linking dopant properties to biochar functionality.

3.7 Rare earth element doping

Recent studies have explored the doping of rare earth elements into carbon materials to enhance their catalytic properties and adsorption capacity (Malavekar et al. 2023; Matskevich et al. 2023; Zhan et al. 2024). Rare earth elements, such as lanthanum (La) and cerium (Ce), are particularly promising due to their unique electronic configurations and ability to form stable complexes with carbon matrices. For example, Wang et al. (2018) demonstrated that La- and Ce-doped biochar possess numerous positively charged hydroxyl groups (≡La–OH, ≡Ce–OH), which exhibit excellent adsorption of phosphate molecules through electrostatic attraction, hydrogen bonding, and inner-sphere complexation (Wang et al. 2018, 2019). This makes rare earth-doped biochar highly effective for applications in water treatment and nutrient recovery. In addition to adsorption, rare earth-doped biochar has shown exceptional potential in catalysis. Yang et al. (2024a; b) designed a Ru-WO_X doped biochar catalyst for the conversion of cellulose to sorbitol (Figure S1). By optimizing the Ru content, they achieved 100% cellulose conversion and an 82.6% sorbitol yield, highlighting the potential of rare earth-doped biochar as a high-performance catalyst. Beyond these applications, rare earth doping can also enhance the thermal stability of biochar, electrical conductivity, and redox activity, making it suitable for advanced energy storage and environmental remediation technologies. For instance, the incorporation of rare earth elements can improve the efficiency of biochar-based supercapacitors and batteries by facilitating faster electron transfer and providing additional active sites for redox reactions (Luo et al. 2024). These findings underscore the transformative potential of rare earth element doping in advancing the functionality of biochar across a wide range of applications, from environmental remediation to catalysis and energy storage.

3.8 Multi-element co-doping

Research on single-element doping in biochar has reached limitations, prompting a shift toward multi-element co-doping to achieve synergistic effects. By combining the advantages of multiple elements, co-doping can enhance properties of biochar beyond the sum of its individual components. A key application of multi-element co-doping is reducing the generation of polycyclic aromatic hydrocarbons (PAHs) (He et al. 2019; Liu et al. 2017a, b; Zhao et al. 2019). For example, Hung et al. (2022) reported that N-B co-doped biochar produced fewer PAHs compared to single N or B doping. They attributed this to the synergistic coupling between N and B atoms and the formation of C–N–B bonds, which effectively inhibited PAH generation. However, inappropriate co-doping can lead to negative effects. Sun et al. (2023b) found that N-S co-doped biochar exhibited lower CO_2 adsorption rates than biochar doped with either N or S alone. This was due to the competitive relationship between N and S, where N-containing functional groups interfered with sulfur oxide formation, and sulfur doping disrupted the functionality of N-containing groups. Despite its potential, the selection of co-doping elements, methods, and mechanisms remains poorly understood. Additionally, evaluating co-doped biochar based solely on the effects of individual elements is insufficient. Further research is needed to explore the complex interactions and synergistic mechanisms in multi-element doped biochar (Roldán et al. 2015).

4 Properties of element-doping biochar

4.1 Surface morphology

Elemental doping significantly influences the morphology of biochar, with different elements imparting distinct structural and surface characteristics. After pyrolysis, doped elements are typically uniformly distributed on the biochar surface, as illustrated Fig. 4a – 4c. However, the specific effects of doping vary depending on the element introduced. For instance, N doping increases the surface roughness and specific surface area of biochar (Fig. 4d – 4f). The result should be attributed to the introduction of N disturbs the decomposition path of the carbon skeleton and intervenes the orderly arrangement of

carbon, which prompts the formation of new microporous structure (Anum et al. 2024; Chen et al. 2019; Rong et al. 2024). Similarly, P doping results in a rougher surface and an irregular carbon structure. During pyrolysis, P not only forms unique phosphide particles on the biochar surface but also alters the rate and extent of carbonization, affecting the cohesion and growth of the carbon matrix (Fig. 4g – 4i) (Zhou et al. 2022b). In contrast, O and S doping tend to create more micropores and increase the specific surface area, as these elements are often released as volatile gases during pyrolysis. Additionally, O and S form abundant functional groups on the biochar surface, which serve as active sites for pollutant degradation (Wang et al. 2022; Yu et al. 2022). Unlike non-metals, metal doping typically results in the formation of metallic compounds that coat the biochar surface. For example, Mg doping leads to the aggregation of magnesium oxide particles on the interior or surface of the biochar (Biswas et al. 2024; Wang et al. 2022). In the case of multi-element doping, the effects on biochar morphology are not simply additive but often synergistic (Fig. 4j – 4 k). For instance, Ahmad et al. (2023) reported that N-Fe co-doped biochar exhibited more pore structures and spherical particles compared to Fe-doped biochar alone, significantly enhancing its capacity for adsorbing refractory organic pollutants.

4.2 Pore structure

Pore size structure is a critical factor influencing biochar performance, and elemental doping serves as an effective modification method to significantly alter its pore characteristics, thereby enhancing its application potential (Zuo et al. 2021). As shown in Table 2 and Fig. 5a, the effects of different doping elements on the pore volume and diameter vary, with most elements increasing the specific surface area (Sun et al. 2024a; b). For instance, alkali metal doping, such as potassium (K), induces structural swelling during pyrolysis due to the interaction between K^+ ions and carbon or functional groups, leading to increased pore size (Luo et al. 2023). In contrast, transition metal doping (e.g., Fe, Cu, Zn) exhibits a dual effect. While metal–organic complexes or metal oxides generated during pyrolysis may block some pores, the growth of these compounds at higher temperatures can also create new pore channels, altering pore size distribution (Song et al. 2024). Non-metallic elements, such as N and S, primarily influence pore structure through chemical reactions. For example, N doping forms nitrogen-containing functional groups (e.g., pyridinic-N, pyrrolic-N), which often results in the formation of micropores and mesopores, enhancing surface area and adsorption capacity (Wang & Wang 2019); while S doping introduces sulfur-containing groups (e.g., thioether, thiophene), which can create hierarchical pore structures, improving accessibility to active sites for catalytic and adsorption processes (Hassaan et al. 2024). Despite these advancements, current research has limitations. The effects of multi-element synergistic doping on pore size remain underexplored, and the quantitative relationship between doping elements and pore size changes is not yet fully understood. Addressing these gaps will be crucial for optimizing biochar performance in environmental and energy applications.

4.3 Degree of graphitization

The degree of graphitization in biochar, reflecting the ordering of carbon atoms into a graphite-like structure, is measured using techniques such as Raman spectroscopy (D/G ratio), X-ray diffraction (XRD) (interlayer spacing d002 and crystallite size Lc), and transmission electron microscopy (TEM) (direct visualization of graphitic layers). Elemental doping can effectively regulate the graphitization degree of biochar, which determines the conductivity, stability, and catalytic performance of biochar (Fu et al. 2023b; Gao et al. 2023a, b; Liao et al. 2024). The effect caused by doping of some elements on the degree of graphitization of biochar is shown in Table S4 and Fig. 5b. For the non-metallic element, taking N as an example, it can be doped into the carbon lattice of biochar to change the distribution of the electron cloud of carbon, which affects the arrangement of carbon atoms and the crystallization process and promotes the reorganization of carbon structure. Eventually, more defects and active sites appear in biochar, disrupting the ordered structure and reducing graphitization (Cheng et al. 2023). However, Gao et al. (2022) pointed out that doping excessive N leads to the formation of more defects and disordered structures in biochar, instead inhibiting the graphitization process. For the metallic element, e.g. iron, cobalt, and nickel, they are doped in biochar for using as catalysts. During pyrolysis, these metal elements can effectively promote the stacking and orderly arrangement of the carbon layers in the biochar by lowering the activation energy required for carbon rearrangement, so that the microstructure in biochar is closer to the graphite structure (Huang et al. 2023a, b; Jia et al. 2018). Besides, the thermal stability of the dopant and its interaction with the carbon matrix also play a role in determining the degree of graphitization. Therefore, doping various elements could regulate the graphitization of biochar, which determines the adsorption properties, stability, mechanical strength, electrical conductivity of biochar, broadening its application fields.

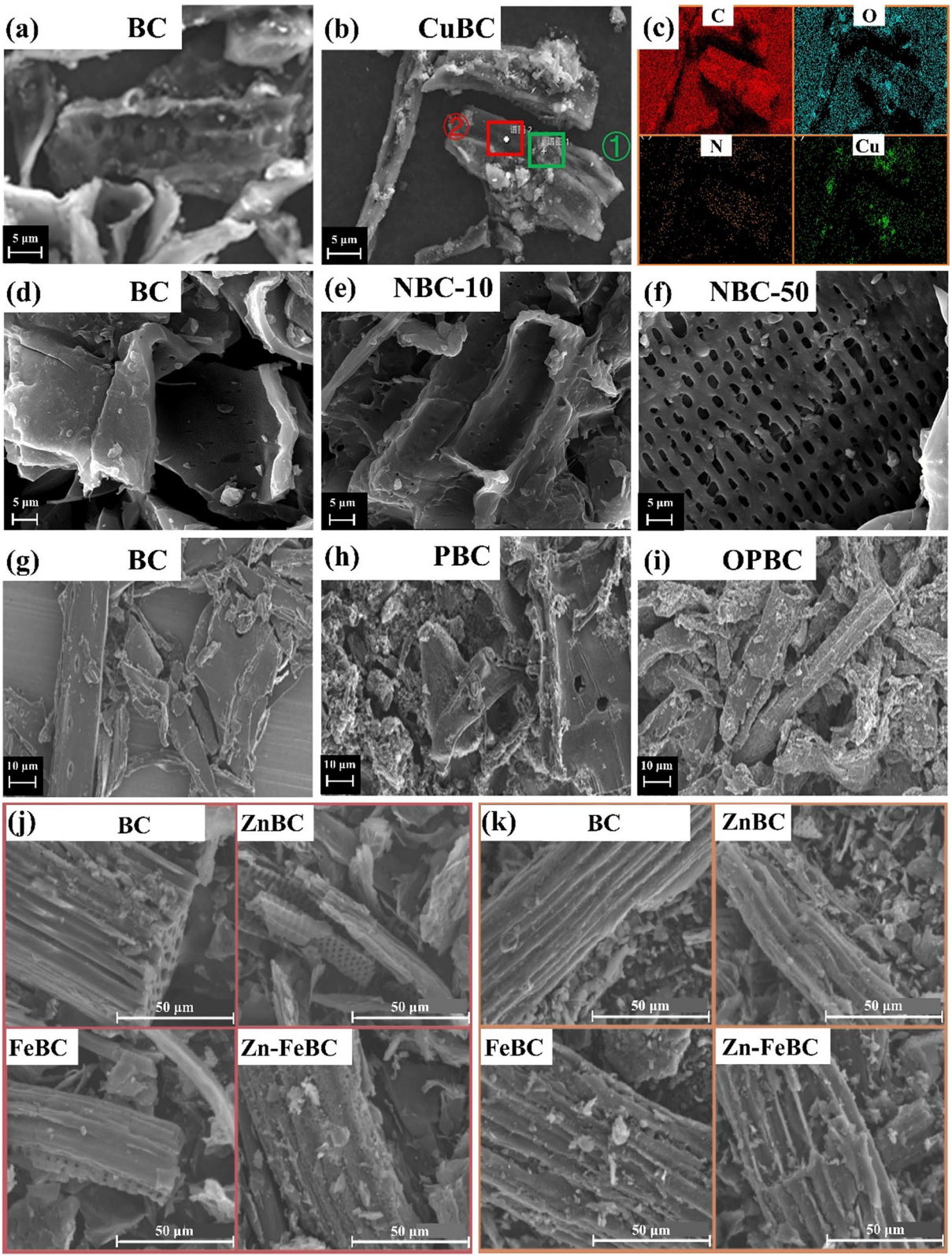

Fig. 4 SEM and EDS images of Cu-doped corn straw-based biochar (**a**–**c**) (Gao et al. 2023a; b); SEM images of N-doped bamboo-based biochar, where 10 and 50 represent the concentrations of the dopant NH_3 (**d**–**f**) (Chen et al. 2020); SEM images of O and P-doped sawdust-based biochar (**g**–**i**) (Wang et al. 2022); SEM images of Fe and Zn-doped corn straw-based biochar (**j**) (Zhou et al. 2023); SEM images of Fe and Zn doped cotton straw-based biochar (**k**) (Zhou et al. 2023)

Table 1 Summary of research progress in element-doped biochar fields

Scope	Novelty	Focused problem	References
Nitrogen self-doped biochar	Related to the development and application of nitrogen self-doped biochar technology	1. Preparation: pyrolysis, gasification, co-pyrolysis 2. Modification: chemical, physical, mineral oxide impregnation, magnetic modification, pre-carbonization 3. Influence factor: effect of feedstock and pyrolysis parameters 4. Application: adsorption, catalytic, capacitive properties and electrochemical, agricultural improvement, environmental impacts	Ruan et al. (2025)
Various element doped biochar	Research progress on the catalysis of ozone by biochars doped with different elements	1. Doping types: metal doping, nonmetal doping 2. Doping methods: external doping and internal doping, co-doping of metal and non-metal elements, green material synthesis methods 3. Application: catalytic oxidation degradation of organic pollutants 4. Economic cost	Zhao (2025)
Sulfur doped biochar	Multidimensional and critical review focus on the formation, determination, synthesis, transformation mechanism, and application of S-functional groups in biochar	1. Determination method 2. Influence factor: feedstocks, pyrolysis temperature 3. Doping methods: S-impregnation, plasma treatment 4. Application: adsorption of heavy metal, solid acid and catalyst, adsorption of CO_2, electrochemical applications, growth of plants and crops	Leng et al. (2022)
N-doped biochars	Critical and comprehensive review is conducted to scrutinize the interspecies transformation of N-dopants in relevant engineering applications	1. Fabrication: endogenous and external N 2. Application: adsorptive removal of pollutants, advanced oxidation processes, energy storage and conversion 3. Limitations in environmental and energy applications	Wan et al. (2020)
Heteroatom co-doped biochar composites	Deep review about introducing metal and heteroatoms into biochar for removing contaminants in water treatment	1. Fabrication: endogenous and external doping 2. Application: heavy metal, organic contaminants 3. Removal mechanisms of contaminants: physical adsorption, ion-exchange, electrostatic attraction, precipitation, surface complexation, oxidation and reduction 4. Influencing factors: physicochemical properties, pH, co-existing substances	Liu et al. (2022)
Heteroatom-doped biochar	Adsorption CO_2 mechanism and methods of heteroatom doping are summarized	1. Adsorption CO_2 mechanism after doping different elements: nitrogen, boron, sulfur, phosphorus 2. Adsorption CO_2 mechanism with different doping methods: pre-decoration, post-decoration	Sun et al. (2024a, b)
Nitrogen-doped biochar	A specific review on adsorptive and oxidative remediation of ROPs using N-doped and Fe/N co-doped BCs	1. N precursors: melamine, urea, cyanamide and dicyandiamide, chitosan 2. Manufacture: co-pyrolysis, hydrothermal carbonization, HTC-pyrolysis, post-modification of BC, green synthesis 3. Distribution of N and Fe species 4. Adsorption and activation oxidation mechanisms of ROPs	Ahmad et al. (2023)
Nitrogen-doped biochar	Comprehensive review on various nitrogen-doped biochar materials	1. Preparation method: one-step method and two-step method, in situ nitrogen mixing and post-treatment nitrogen mixing 2. Application: catalysis, adsorption of pollutants, supercapacitor	Feng et al. (2024a, b)

Table 1 (continued)

Scope	Novelty	Focused problem	References
Zero Valent Iron -doped biochar	Comprehensive systematic reviews that explain the influence of BC on ZVI formation in terms of the structural characteristics of biochar	1. Structure: surface chemical properties, 2. Preparation methods: pyrolysis-liquid phase reduction method, one-pot synthesis method, ball-milling method, hydrothermal carbonization method, green synthesis method 3. Application: contaminant removal 4. Ecotoxicity: animal, microbiological, plant	Li et al. (2023a, b, c)
Element-doped biochar	Providing a systematic and comprehensive review of element-doped biochar, focusing on its preparation methods, structural properties, enhanced functionalities, and diverse applications	1. Element doping mode: in situ doping, exogenous doping 2. Types of doping elements: nitrogen, oxygen, sulfur, phosphorus, halogen, metal, rare earth element, multi-element 3. Properties: surface morphology, pore structure, degree of graphitization, surface crystal compositions, surface chemical properties 4. Application: soil enhancement, carbon storage, emission mitigation, adsorption, catalysis, and energy storage, cosmetics and bio-composites	This study

Table 2 Pore structure of biochar partially blended with different elements

Biochar source	Dopant	S_{BET} ($m^2\ g^{-1}$)	V_{pore} ($cm^3\ g^{-1}$)	D_{avg} (nm)	References
Wheat straw 800 °C	Untreated	202.3	0.18	2.80	Li et al. (2020)
	N	258.2	0.20	3.16	
	Fe	250.4	0.26	4.14	
	N-Fe	362.5	0.30	3.28	
Sawdust 800 °C	Untreated	75.6	0.17	NA[b]	Xu et al. (2020)
	N	174.4	0.20	NA	
Juniper chips 900 °C	Untreated	670.0	0.34	2.12	Lin et al. (2023a, b)
	N	841.0	0.63	3.02	
Wheat straw 600 °C	Untreated	38.4	0.05	8.44	Yang et al. (2023a, b)
	Fe–Mn	186.7	0.17	7.13	
Wheat straw 900 °C	Untreated	2.11	0.01	23.82	Kong et al. (2023)
	Fe	14.9	0.02	5.97	
	Ni	30.7	0.07	9.44	
	Zn	68.6	0.06	3.73	
Wood chip 600 °C	Untreated	86.7	0.16	7.40	Liu et al. (2023)
	Mn-N	395.2	0.27	2.70	
Orange 500 °C	Untreated	17.85	0.04	2.18	Sun et al. (2023e)
	Fe-Cu	56.54	0.03	4.65	
Phragmites australis 600 °C	Untreated	111.20	0.19	6.98	Wang et al. (2018)
	Fe	232.69	0.28	4.78	
	La-Fe	287.11	0.23	3.13	
Bamboo 500 °C	Untreated	2.06	6.13×10^{-3}	11.90	Talukdar et al. (2020)
	Fe	2.89	1.43×10^{-2}	19.80	
	Ag-Fe	4.28	4.42×10^{-2}	41.40	
Bamboo 900 °C	Untreated	593.2	0.12	2.97	Huang et al. (2020)
	Mn-Fe	364.6	0.33	4.33	
Corn stalks 900 °C	Untreated	322.4	0.29	NA	Yang et al. (2023a, b)
	N-B	607.1	0.41	NA	
Collagen fiber 800 °C	Untreated	716.0	0.58	NA	Guo et al. (2023)
	Fe	893.4	3.06	NA	
	Co	1247.5	0.64	NA	
	Fe-Co	2097.7	0.84	NA	
Pine needles 600 ~ 800 °C	Untreated	115.4	0.06	1.12	Zhang et al. (2022a)
	N-S	372.9	0.31	1.13	
Bamboo 240 °C (hydrothermal)	Untreated	7.0	0.02	NA	Zhang et al. (2022b)
	O	1386.0	0.10	NA	
Peanut shell 900 °C	Untreated	283.1	0.11	2.37	Jin et al. (2022)
	Fe-S	345.2	0.16	2.18	
Edible mushroom 700 °C	Untreated	18.6	0.09	20.18	Bai et al. (2022)
	Zn-Mo	113.17	0.39	13.83	
Chitosan 800 °C	Untreated	1.4	NA	NA	Qi et al. (2022)
	Fe-Cu	209.7	NA	9.42	
Waste wood 800 °C	Untreated	272.0	0.02	4.21	Zhou et al. (2022a)
	P	895.5	1.00	4.64	
Wheat straw 900 °C	Untreated	63.3	0.031	NA	Liu et al. (2020a, b)
	B	22.6	0.026	NA	
	K	1358.4	0.65	NA	
	B-K	1189.9	0.57	NA	

Table 2 (continued)

Biochar source	Dopant	S_{BET} ($m^2\ g^{-1}$)	V_{pore} ($cm^3\ g^{-1}$)	D_{avg} (nm)	References
Bacillus megaterium 900 °C	Untreated	73.1	0.08	4.61	Zhang et al. (2021)
	Se	36.8	0.06	6.23	
	N	148.3	0.05	3.55	
	Se-N	287.3	0.07	3.01	

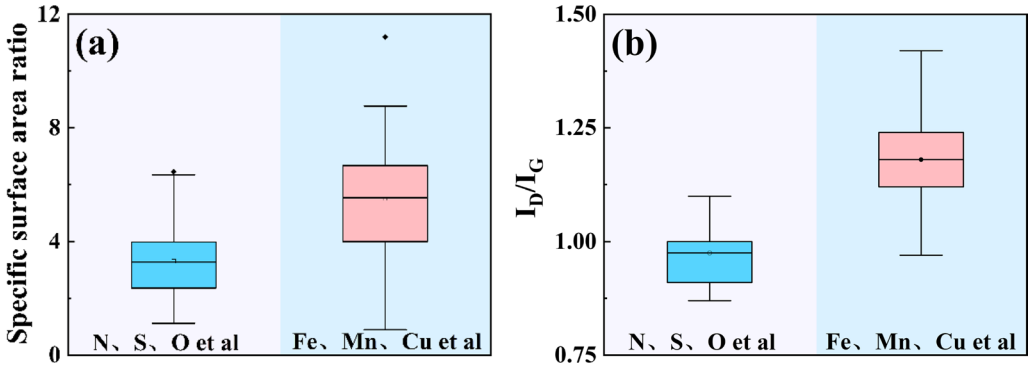

Fig. 5 Specific surface area ratio after elemental doping (Data from Table 2) (**a**). Differences in I_D/I_G of element-doped biochar (Data from Table S4) (**b**)

4.4 Surface crystal compositions

The surface crystal composition of biochar is significantly influenced by elemental doping, which plays a critical role in determining its properties, such as adsorption capacity, catalytic activity, and electrical conductivity (Aziz et al. 2023; Zhan et al. 2024). The effects of doping vary depending on the type of element introduced. For instance, doping with transition metals (e.g. iron and copper) and non-metallic elements (e.g. nitrogen) can introduce defects and distortions in the crystal structure of biochar (Figure S2). For example, Xu et al. (2025) observed that Fe-doped biochar derived from coffee grounds exhibited significant changes in its amorphous carbon structure at 24° and 43°, which enhanced its adsorption capacity for chloroquine phosphate. Similarly, Fu et al. (2023b) found that nitrogen doping into the carbon skeleton to form carbon nitride crystals often results in non-uniform bonding patterns and ratios between nitrogen and carbon atoms, leading to defects such as vacancies and dislocations in the crystal structure.

In contrast, alkali metals (e.g., sodium and potassium) and mineral phosphorus influence the growth and orientation of surface crystals (Figure S2). For example, Liu et al. (2024) reported that potassium ions adsorbed onto the growth surface of calcium carbonate crystals alter their growth rate and orientation, resulting in the formation of $CaKPO_4$ crystals with unique morphologies. Additionally, phosphorus forms stable chemical bonds with carbon and silicon in the surface crystals of biochar. Liang et al. (2022) demonstrated that the formation of Si-P chemical bond in SiP_2O_7 crystals not only enhances the adsorption of 2,4-dichlorophenoxyacetic acid but also increases the stability of the surface crystals of biochar.

4.5 Surface chemical properties

The surface of biochar is rich in diverse functional groups, including carboxyl (–COOH), hydroxyl (–OH), carbonyl (C=O), phenolic hydroxyl, and ether (C–O–C) groups. These groups impart chemical reactivity of biochar, enabling it to engage in adsorption, ion exchange, complexation, and other environmental reactions (Fan et al. 2021). Elemental doping allows for targeted adjustments to these functional groups, enhancing the performance of biochar to meet the demands of various applications. For example, N-doped biochar exhibits distinct absorption peaks for pyridine-N and pyrrole-N functional groups (Fig. 6a), significantly boosting its catalytic and adsorption abilities (Chen et al. 2019; Gao et al. 2022). O-doped biochar introduced hydrophilic groups (e.g., –OH, C=O), enhancing reactivity, adsorption capacity for polar pollutants, and catalytic activity (Yang et al. 2020). Similarly, S-doped biochar incorporated acidic and redox-active groups (e.g., C–S, S=O), improving heavy metal adsorption and electrochemical performance for

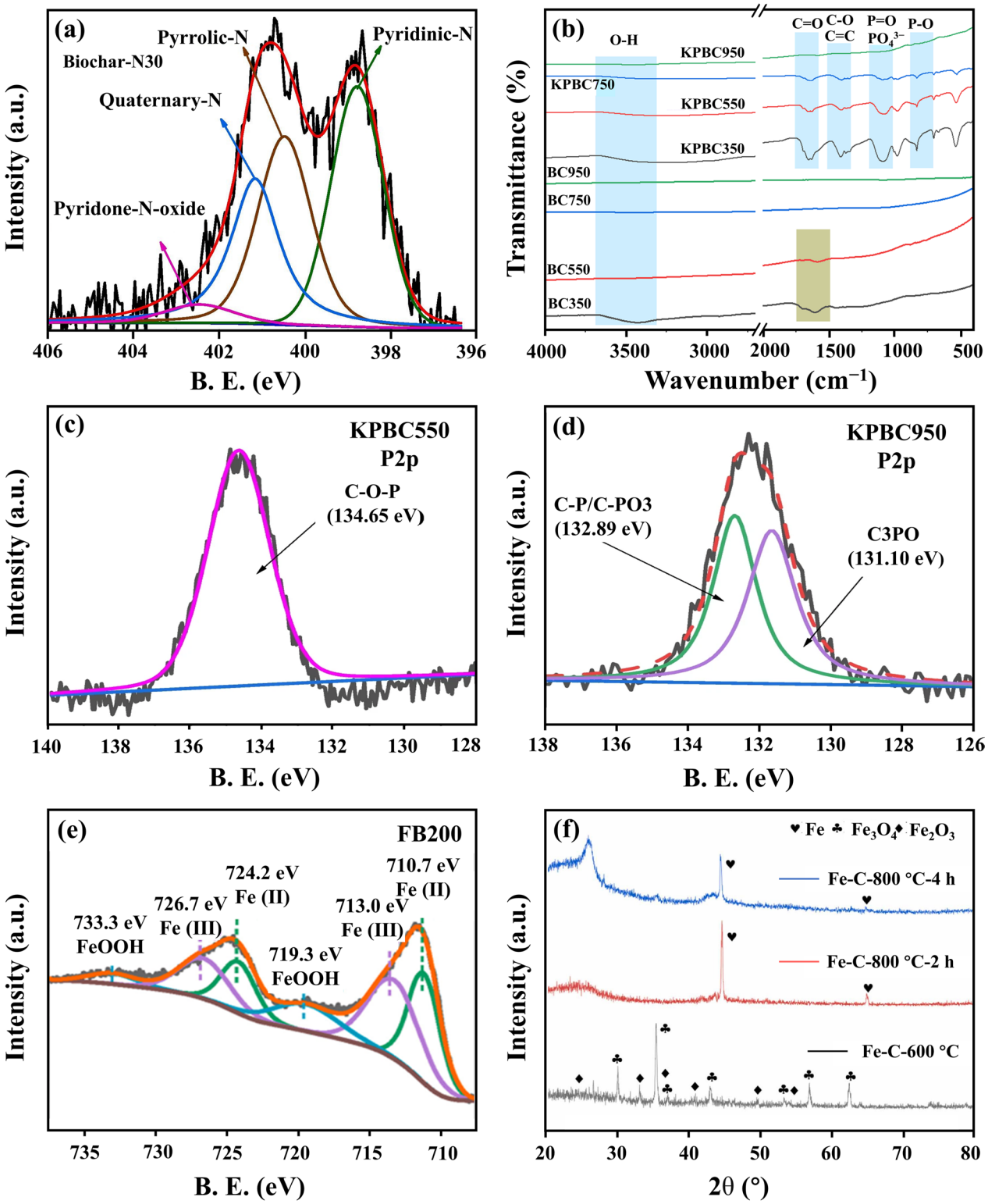

Fig. 6 XPS of N-doped biochar (**a**) (Chen et al. 2019); FTIR and XPS of P-doped biochar (**b**–**d**) (Sun et al. 2024a, b); XPS of Fe-doped biochar (**e**) (Tian et al. 2023); XRD of Fe-doped biochar (**f**) (Yang et al. 2024a, b)

energy storage (Leng et al. 2022). P-doped biochar shows prominent peaks for phosphate functional groups (e.g., P=O, PO_4^{3-}, P–O, C–O–P, C–P, C–PO_3) (Fig. 6 b – 6d). The P2p orbitals in XPS spectra further reveal the presence of C–O–P (Fig. 6c – 6d), which contribute to the stability and adsorption capacity of biochar (Wang et al. 2023b; Yang et al. 2024a, b; Yu et al. 2022). In the case of metal doping, elements such as Fe and Cu can react with functional groups during pyrolysis (Fig. 6e – 6f). For instance, Fe-doped biochar forms new $Fe(COOH)^{2+}$ complexes on its surface (Formula 5) (Jia et al. 2021; Ahmad et al. 2024). Therefore, it is expected to realize the precise regulation of the functional groups by doping specific element in biochar.

$$Fe^{3+} + -COOH \rightarrow Fe(COOH)^{2+} + H^{+} \quad (5)$$

5 Application of element-doped biochar

As elemental doping technology for biochar continues to advance, biochar with tailored properties is being increasingly applied across diverse fields. By doping biochar with specific elements, it is possible to induce unique functionalities that are absent in untreated biochar. According to existing literature, element-doped biochar is primarily utilized in soil enhancement, carbon storage, emission mitigation, adsorption, catalysis, and energy storage systems (Table 3).

5.1 Soil improvement agent

Biochar is widely recognized for its ability to enhance soil quality, sequester carbon, and remediate soil heavy metal pollution, making it a promising tool for improving soil health (Fig. 7 and Table S5) (Chen et al. 2018; Mujtaba Munir et al. 2021). However, excessive use of biochar can lead to unintended negative effects, such as decreasing microbial diversity, the introduction of PAHs, and alterations in soil pH, potentially causing secondary soil pollution (Yang et al. 2022a, b). To mitigate these challenges, recent studies have focused on improving biochar through the doping of soil-friendly elements (e.g., P, N, K), which not only minimize adverse effects but also enhance its beneficial properties (Mašek et al. 2019). For example, N and B co-doped biochar has been shown to introduce nitrogen- and boron-containing functional groups, which reduce unstable carbon structures and decrease PAH residues, thereby addressing concerns about secondary pollution (Hung et al. 2022). Additionally, biochar doped with elements such as N, S, K, Mg, Ca, and P could supplement essential nutrients for soil, promoting plant growth and improving soil fertility. K-doped biochar has been found to enhance soil structure by promoting the formation of stable soil aggregates. It also increases soil pH, cation exchange capacity (CEC), anion exchange capacity (EC), and soil organic matter (SOM), which collectively improve water infiltration, root growth, and soil aeration (Da et al. 2023). P-doped biochar serves as a habitat for beneficial microorganisms, such as bacteria and fungi, which play critical roles in nutrient cycling, organic matter decomposition, and soil respiration, thereby enhancing overall soil health (Li et al. 2022a, b). These findings demonstrate that element-doped biochar not only addresses the limitations of conventional biochar but also introduces additional benefits, such as nutrient supplementation, improved microbial activity, and enhanced soil structure. By optimizing the doping process and selecting appropriate elements, biochar can be tailored to meet specific soil improvement needs, making it a versatile and sustainable solution for soil remediation and agricultural enhancement.

5.2 Adsorbent and catalyst carrier

Adsorbent. Biochar is widely recognized for its exceptional adsorption capabilities (Table S6), which are further enhanced by doping with various elements. Doping modifies the surface chemistry, functional groups, specific surface area, and pore structure of biochar, making it highly effective for removing contaminants such as heavy metals, organic pollutants, and volatile organic compounds (VOCs) (Chen et al. 2019; Lu et al. 2023; Rajapaksha et al. 2016; Wu et al. 2022). For instance, Lina et al. (2024) found that Cu-doped biochar could remove specific heavy metal ions (e.g. Hg^{2+}) by hydrogen bonding, electrostatic attraction, or displacement reactions. Cheng et al. (2022) selected melamine as N source for preparing N-doped biochar, and found that it could significantly degrade volatile organic compounds (VOCs) using abundant N-containing functional groups on its surface through π-π dispersion, hydrophobic and electrostatic interactions. Mian et al. (2018) prepared N-Fe co-doped biochar, and found that new N-containing functional groups and dispersed iron oxides particles appeared on its surface. The former could adsorb Cr (VI) via electrostatic interactions, while the later converted Cr (VI) to Cr (III) via redox reactions. The adsorption mechanisms of element-doped biochar include pore-filling, hydrogen bonding, acid–base interactions, chelation, π-π stacking, hydrophobic interactions, and electrostatic interactions, as summarized in Fig. 8a–c and Table S6 (Hu et al. 2024; Li et al. 2023a, b, c; Mayilswamy et al. 2023; Wang et al. 2024; Yuan et al. 2023a, b; Zhang et al. 2023a, b).

Catalyst carrier. The unique properties of biochar, such as its high surface area, porous structure, and tunable surface chemistry, make it an excellent catalyst carrier.

Table 3 Characterization by doping with different elements and its related applications

Dopant	Performance	Key applications	Relevant mechanisms	References
Nitrogen	Electron-rich properties, improved surface alkalinity	Carbon dioxide capture, selective catalytic reduction of nitrogen oxides	High electronegativity, nitrogen-containing active sites	Chen et al. (2015) Li et al. (2019)
Phosphorus	Acid–base properties, enhanced adsorption capacity	Heavy metal removal, organic pollutant degradation	Introduction of phosphate groups, acids: exchange, complexation; bases: electrostatic, precipitation	Li et al. (2022a, 2022b)
Sulfur	Redox activity, improved conductivity	Energy storage devices (e.g. lithium-sulfur batteries), fuel desulfurization	Altered electronic structure of biochar, Sulfur participates in the reaction as an active substance	Wang et al. (2016a, b, c) Cho et al. (2022)
Chlorine	Sterilization and disinfection, promotion of certain reactions	Water treatment, organic synthesis	Strong oxidizing properties, chlorine is highly electronegative, can be used as a halogenating agent	Haoming et al. (2022) Jannis et al.(2024)
Iron	Magnetic, catalytic activity	Environmental remediation, catalysis	Iron confers magnetic properties and iron atoms can act as catalytic activity centers	Wang et al. (2016a, b, c)
Zinc	Antibacterial, anti-inflammatory, tyrosinase inhibition	Cosmetics, skin care, water purification	Zinc ions bind to enzymes, proteins, etc. and affect their activity, removal of impurities by adsorption and precipitation	Caron et al. (2024)
Silver	Strong antimicrobial, conductive properties	Medical equipment, electronic materials	Binds to bacterial sulfhydryl groups and kills them, reducing resistance and improving device performance	Siddiqui et al. (2017)
Nickel	High temperature stability, catalytic activity	Catalytic conversion of biomass, fuel cells	Filling the lattice structure to enhance stability and acting as active sites to reduce reaction activation energy	Zhu et al. (2017) Ambursa et al. (2020)

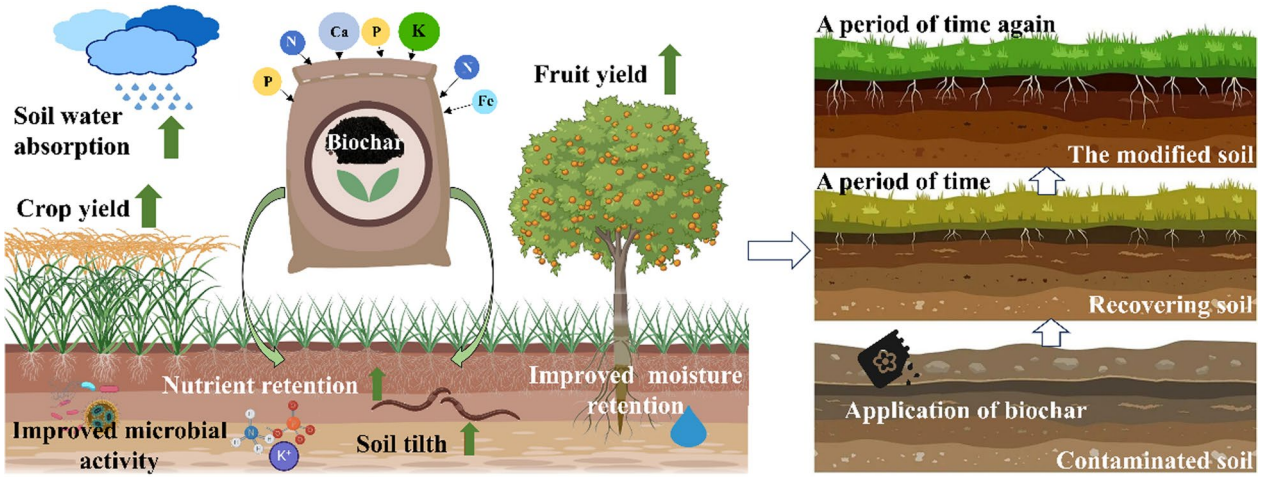

Fig. 7 Soil improvement by elementally doped biochar. Adapted from Yameen et al. (2024)

Doping with elements like nitrogen, iron, and oxygen enhances its catalytic performance by introducing active sites, improving electron transfer, and optimizing surface reactivity (Mahesan et al. 2023). For instance, N-doped biochar owned amphiphilicity, smaller size, superior graphite structure, which made it efficiently degrade

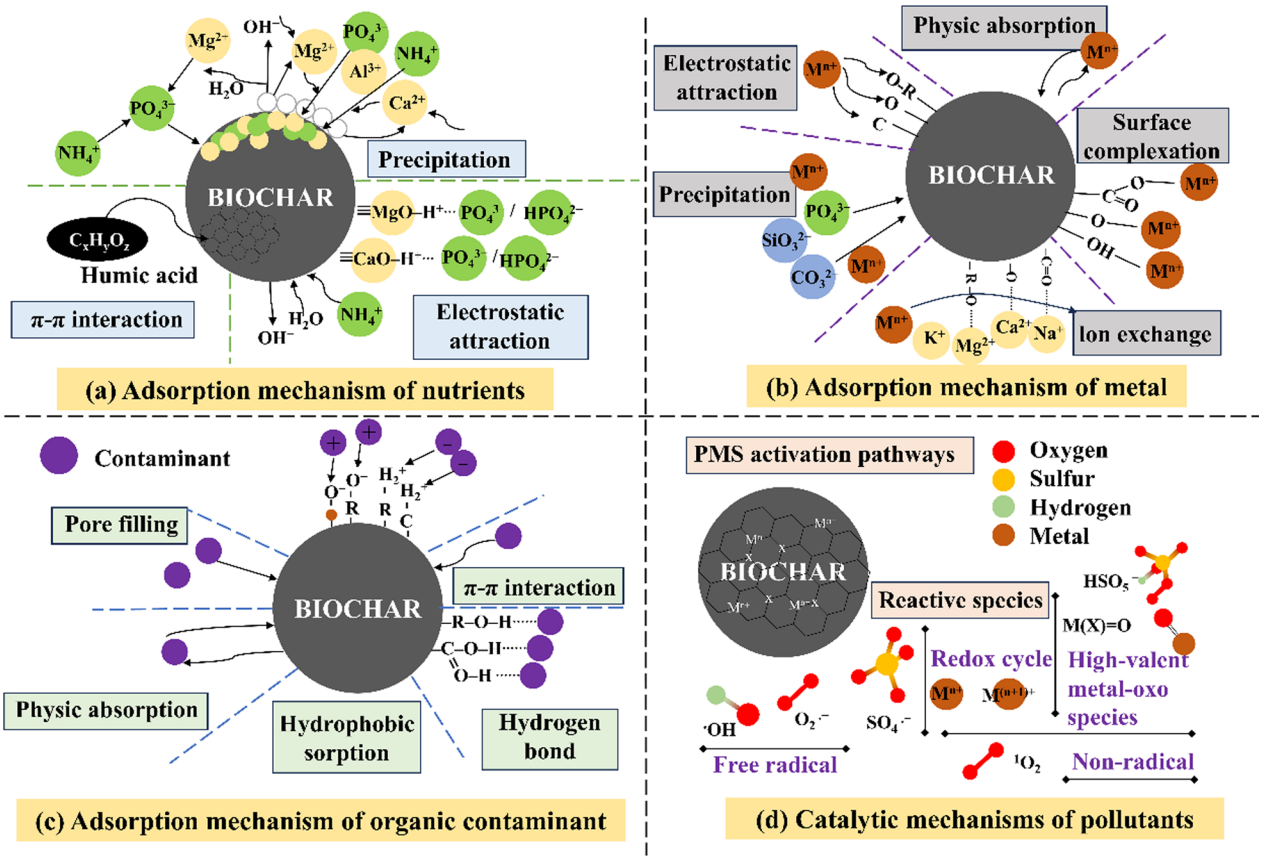

Fig. 8 Main mechanisms of pollutant elimination by element-doped biochar. Manickavasagam et al. (2024) Adapted from Rakesh et al. (2023), Yameen et al. (2024)

pyrene (PYR) into small molecules, such as phenol and benzoic acid, CO_2, and H_2O. These small molecules then were transferred and diffused out of the soil through the small pore structure (Wang et al. 2024). Fe and O co-doped biochar, featuring unique C–O–Fe bonds and abundant aryl rings, achieves complete elimination of tetracycline through π-π stacking and redox reactions (Tao et al. 2024). Doped biochar serves as a versatile catalyst carrier, facilitating reactions such as redox processes, hydrolysis, and advanced oxidation (Chen et al. 2022; Manickavasagam et al. 2024). The catalytic mechanisms are further detailed in Fig. 8d and Table S6.

Despite their distinct applications, element-doped biochar used as an adsorbent and catalyst carrier shares several common characteristics: (1) high surface area and porosity could enhance contaminant adsorption and provide active sites for catalytic reactions; (2) tunable surface functional groups (e.g., −OH, C=O, C–O–Fe) improve interactions with target molecules and facilitate redox reactions; (3) excellent electron transfer properties are crucial for both adsorption (e.g., electrostatic interactions) and catalysis (e.g., redox reactions); and (4) shared mechanisms such as π-π stacking, electrostatic interactions, and redox reactions are applicable in both processes. These shared traits make doped biochar a highly versatile material for environmental remediation and catalytic applications.

5.3 Sequestrating carbon

Biochar is widely recognized as a promising method for carbon sequestration and greenhouse gas mitigation, offering a sustainable solution to combating climate change (Nguyen et al. 2023). During pyrolysis, carbon in biowaste undergoes decomposition, polymerization, and carbonization, forming stable aromatic groups and highly polymerized carbon structures (Yang et al. 2021). However, in traditional biochar, only about 50% of the carbon from biowaste develops a relatively stable structure, limiting its carbon sequestration potential (Leng et al. 2019; Zimmerman 2010). To address this limitation, recent studies have demonstrated that element doping can significantly enhance the carbon sequestration capacity of biochar (Table 4 and Figure S3). For instance, alkali metal-doped biochar (K, Na, Ca, and Mg) has shown improved carbon stability, with Mg-doped biochar exhibiting the highest carbon sequestration efficiency. This enhancement is attributed to the physical protection provided by metal oxides on the biochar surface and the chemical bonding within the carbon matrix, which collectively reduce carbon loss during pyrolysis (Nan et al. 2020). Similarly, Si-doped biochar forms a unique C–Si structure, where silicon acts as a protective barrier to hinder carbon loss, further improving carbon stability (Xiao et al. 2014). Phosphorus-doped biochar demonstrates exceptional thermal stability, with an initial thermal decomposition temperature 100–200 °C higher than that of untreated biochar. Additionally, the mass loss rate of P-doped biochar is reduced by 15 ~ 30% in the high-temperature range of 600 ~ 800 °C, owing to the formation of stable C–P bond and a more ordered carbon layer structure (Yang et al. 2024a; b). Furthermore, N-doped biochar enhances carbon sequestration through the formation of protective films on its surface. The abundant N-containing functional groups (e.g., amino groups) interact with microbial cell surfaces, reducing microbial degradation of biochar and indirectly inhibiting carbon loss (Anum et al. 2024; Zhao et al. 2023). The mechanisms by which element doping enhances carbon sequestration can be categorized into three primary pathways: chemical bonding, physical barriers, and the absorption of carbon molecules during pyrolysis (Fig. 9). Chemical bonding encompasses various types, including nonmetal covalent bonds, metal covalent bonds, π covalent bonds, and organometallic bonds (Shao et al. 2021; Wu & Radovic 2006). Metallic and nonmetallic dopants can form stable heteroatom-C covalent bonds and organometallic bonds with carbon in biomass, thereby effectively minimizing carbon loss during pyrolysis (Wu et al. 2022). Additionally, π covalent bonds can link two planar carbon rings, which enhances the stability of the carbon structure (Hu et al. 2014). Metal oxides (e.g., CaO, MgO) formed during pyrolysis act as physical barriers, reducing volatile carbon loss and preserving carbon within the biochar matrix (Nan et al. 2020). Meanwhile, these metal oxides can absorb and combine with small carbon molecules produced during pyrolysis, forming stable compounds that further enhance carbon retention (Guo et al. 2020a, b), as shown in Formulas 6, 7, 8, 9.

$$BaO(s) + CO_2(g) \rightarrow BaCO_3(s) \quad (6)$$

$$CaO(s) + CO_2(g) \rightarrow CaCO_3(s) \quad (7)$$

$$MgO(s) + CO_2(g) \rightarrow MgCO_3(s) \quad (8)$$

$$MgO(s) + Na_2CO_3(s) + CO_2(g) \rightarrow Na_2Mg(CO_3)_2(s) \quad (9)$$

5.4 Storing energy

Incorporating impurity elements into biochar has emerged as a highly effective strategy for enhancing their energy storage capacity. Element doping introduces additional defects, active sites, and functional groups, which

Table 4 Effect of different elements on biochar yield and carbon retention during pyrolysis

Biochar source	Dopant	Carbon retention (%)	Biochar yield (%)	References
Sewage sludge 300 ~ 700 °C	/	71.6 ~ 41.6	80.4 ~ 67.9	Ren et al. (2018)
	Ca	75.2 ~ 38.8	82.3 ~ 68.0	
Cattle manure 500 °C	/	50.0	30.4	Nan et al. (2020)
	K	54.3	43.5	
	Na	56.2	44.0	
	Mg	65.7	38.3	
	Ca	64.6	42.4	
Spruce sawdust	/	46.6	28.2	Nurgül et al. (2023)
400 °C	Si	55.5	30.2	
Pine sawdust 500 °C	/	46.5	31.3	Zhao et al. (2017)
	P	73.9 ~ 78.5	50.6	
Miscanthus 350 ~ 750 °C	/	About 40.1 ~ 23.3	About 21.5 ~ 17.3	Mašek et al. (2019)
	K	About 47.3 ~ 28.2	About 26.4 ~ 21.2	
Sewage sludge 350 ~ 600 °C	/	80.0 ~ 43.0	/	Shen et al. (2020)
	Fe	90.0 ~ 60.0	/	
Coffee husk 500 °C	/	40.0	33.0	Carneiro et al. (2018)
	P	81.9	65.0	
	P-Mg	69.5	62.0	
Chicken manure 250 ~ 550 °C	/	77.8 ~ 33.9	66.0 ~ 42.5	Xiao & Chen (2017)
	Ca	81.3 ~ 47.2	77.0 ~ 53.0	
	Mg	74.5 ~ 49.6	79.5 ~ 50.5	
Straw 300 ~ 700 °C	/	75.6 ~ 51.9	55.5 ~ 34.5	Liu et al. (2020a, b)
	Al-Si	84.7 ~ 63.0	68.6 ~ 46.6	
Rape straw 800 °C	/	47.7	/	Gao et al. (2018)
	P	53.2	/	

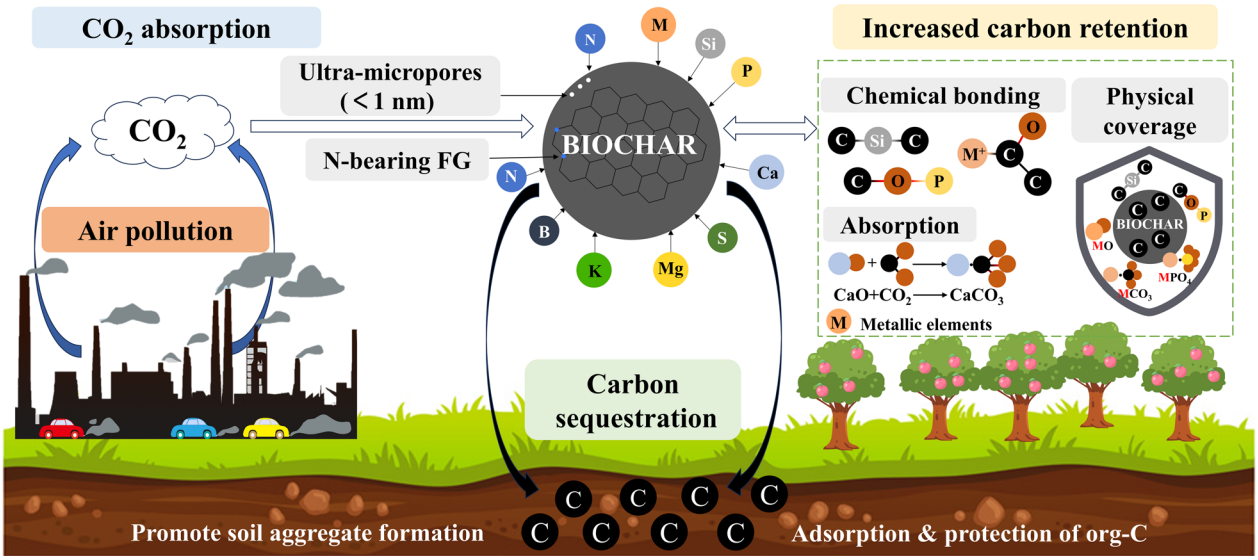

Fig. 9 Carbon sequestration process of element-doped biochar

widen layer spacing, improve charge transfer, enhance electrode/electrolyte interactions, and boost overall energy storage performance. These modifications significantly enhance the electrochemical properties and longevity of energy storage devices, enabling the use of doped biochar in the field of supercapacitors and ion batteries a promising alternative to conventional materials like graphene and carbon nanotubes (Table 5 and Figure S4) (Deng et al. 2020).

Supercapacitors have emerged as leading energy storage devices, and element-doped biochar has shown considerable promise in this field. Key advantages include enhanced specific capacitance, improved electrical conductivity, and superior cycling stability (Radosław et al. 2024). Elements such as nitrogen (N), sulfur (S), and phosphorus (P), which have different electronegativities compared to carbon, can alter the electron cloud distribution and optimize the pore structure of biochar. This creates more charge storage areas and active sites, increasing the specific capacitance of supercapacitors (Makinde et al. 2024). For example, Deng et al. (2020) prepared an N-doped electrode material with a specific capacitance of 159 F g^{-1} at 1 A g^{-1}. They pointed out that heteroatoms like nitrogen can form conjugated π-bonds (e.g., N–C bonds) with carbon atoms, facilitating electron transport, reducing resistance, and enhancing the charging and discharging speeds of supercapacitors. N and B co-doped biochar also significantly boost the specific capacitance of supercapacitors by improving C wettability and conductivity and enabling reversible redox reactions (Wang et al. 2016a, b, c). Additionally, cycling stability is another critical performance metric for supercapacitors. Element doping can improve the structural stability of biochar, minimizing damage during

Table 5 Composition and structure of elementally doped biomass carbon materials and their electrochemical energy storage applications

Feedstock	Doping types and reagents	Doping elements	Topography	Appliance	Electrochemical properties	References
Wax gourd	Self-dopant	N (1.9%)	Porous carbon	SCs	330 mF g^{-1} at 1 mA g^{-1} (6 mol L^{-1} KOH)	Yu et al. (2018)
Gelatine	Exogenous-doping (KNO_3)	N (9.5%)	Porous carbon	SCs	159 mF g^{-1} at 1 mA g^{-1} (6 mol L^{-1} KOH)	Deng et al. (2020)
Spirulina	Exogenous-doping (urea)	N (1.2%), O (13.3%)	Porous carbon	SCs	341 mF g^{-1} at 1 mA g^{-1} (6 mol L^{-1} KOH)	Geng et al. (2023)
Pomelo	Exogenous-doping [$Co[NO_3]_2{\cdot}6H_2O$, potassium ferricyanide, S]	Co, Fe, S	Porous carbon	Li–S	447 m Ah g^{-1} after 500 cycles at 1 A g^{-1}	Jing et al. (2019)
Fish scales	Exogenous-doping (sulfuric)	S (6.2%)	Carbon nanofiber	Li–S	1023 m Ah g^{-1} after 70 cycles at 1 A g^{-1}	Zhao et al. (2013)
Wheat straw	Exogenous-doping (KOH)	N	Porous carbon	LIBs	343 m Ah g^{-1} after 1000 cycles at 1 A g^{-1}	Yan et al. (2019)
Bagasse	Exogenous-doping ($KMnO_4$)	Mn	Porous carbon	LIBs	388 m Ah g^{-1} after 150 cycles at 1 A g^{-1}	Pongpanyanate et al. (2024)
Wheat grain	Exogenous-doping (Si NPs)	N (6.1%)	Carbon nanofiber	LIBs	478 m Ah g^{-1} after 1000 cycles at 1 A g^{-1}	Sun et al. (2023a)
Soybean straw	Exogenous-doping (carboxamide)	N (4.9%)	Carbon nanofiber	ZABs	Power density up to 88.40 mW·cm^{-2}	Meng et al. (2024)
Asparagus	Exogenous-doping [$Co(NO_3)_2$, $Fe(NO_3)_3$]	N (3.9%), Co, Fe	Porous carbon	ZABs	Power density up to 94 mW·cm^{-2}	Miao et al. (2022)
Sodium citrate	Exogenous-doping (urea)	N (6.9%)	Porous carbon	PIBs	384 m Ah g^{-1} after 500 cycles at 0.1 A g^{-1}	Yan et al. (2020)
Acesulfame K	Self-dopant	N (2.5%), S (8.9%)	Porous carbon	PIBs	205 m Ah g^{-1} after 1000 cycles at 0.5 A g^{--1}	Kim et al. (2024)
Chlorella	Exogenous-doping (phosphotungstic acid, sulfur powder)	P, S, N	Porous carbon	PIBs	155 m Ah g^{-1} after 5300 cycles at 1 A g^{-1}	Kang et al. (2020)
Pine chip	Exogenous-doping (N-methylpyrrolidone)	N (2.7%), P (5.5%)	Sheet porous carbon	SIBs	101 m Ah g^{-1} after 1000 cycles at 0.5 A g^{-1}	Yu et al. (2021a, 2021b)
Chlorella	Exogenous-doping (phosphotungstic acid, sulfur)	P, S, N	Porous carbon	SIBs	311 m Ah g^{-1} after 6000 cycles at 3 A g^{-1}	Kang et al. (2021)

charge–discharge cycles. For instance, the S-doped activated biochar (SA-Come electrode) fabricated from camellia (Fig. 10) retains 98% of its capacitance after following 15,000 cycles at 4.0 A g^{-1} (Xia et al. 2022). Geng et al. (2023) developed N, O co-doped biochar that retained 99.2% of its capacitance after 10,000 cycles at a current density of 10 A g^{-1}, demonstrating exceptional stability.

Beyond supercapacitors, element-doped biochar has gained attention in ion batteries and lithium-sulfur batteries (Li et al. 2017a, b; Liu et al. 2018). The performance of lithium-ion batteries depends heavily on the lithium-ion storage capacity and structural stability of the anode material. While pristine biochar has limited storage capacity, elemental doping can significantly enhance this property. For example, Sun et al. (2023a) reported that Si-doped biochar formed a stable nitrogen-containing cladding after annealing, preventing direct contact between silicon nanoparticles and the electrolyte. This resulted in a reversible capacity of 478.0 m Ah g^{-1} after 1,000 cycles at 1 A g^{-1}. Sodium and potassium ions have larger radii than lithium ions, leading to significant volume changes during charge–discharge cycles. Element-doped biochar can mitigate this issue by improving structural and mechanical properties. Kang et al. (2020) developed N, P co-doped biochar that reduced mechanical stress,

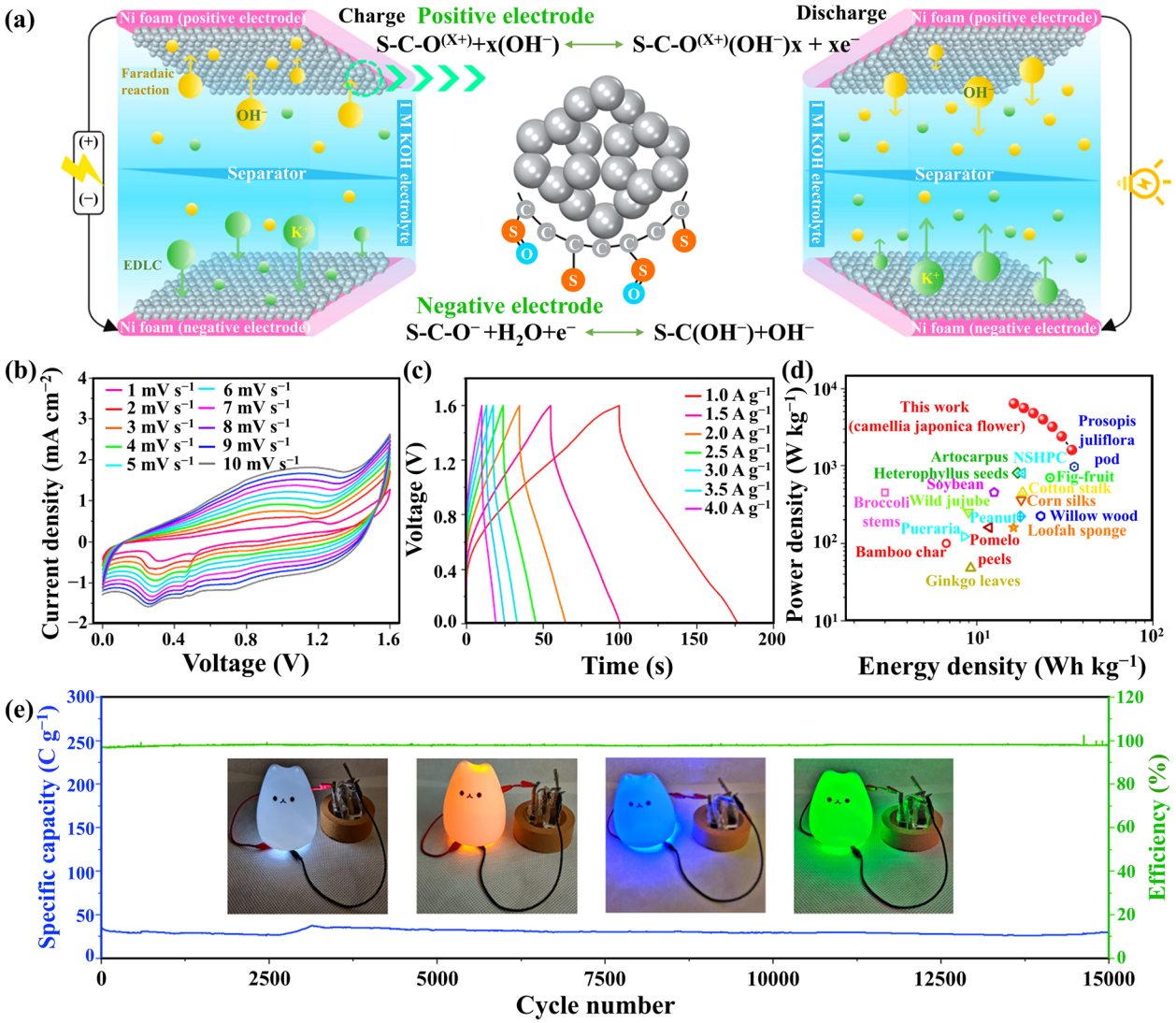

Fig. 10 Charging mechanism diagram of sulfur-doped biochar symmetric supercapacitor (**a**), CV curves of supercapacitors manufactured at different scanning rate (**b**), GCD curves of supercapacitors prepared at different current densities (**c**), Ragone diagram for manufacturing supercapacitors (**d**), Cycle stability and capacitance efficiency of manufacturing supercapacitors (**e**) (Xia et al. 2022)

inhibited volume expansion, and shortened sodium diffusion paths, significantly enhancing battery performance. Additionally, doped elements such as nitrogen and oxygen enhance polysulfide adsorption and mitigate the "shuttle effect," while metallic dopants (e.g., manganese, nickel) catalyze polysulfide conversion. Ju et al. (2023) demonstrated that N, Mn co-doped biochar significantly improved the cycling stability of lithium-sulfur batteries. However, the application of elementally doped biochar in energy storage still faces some challenges, including insufficient research on the doping mechanism and structure–property relationship, the scale-up and controllability of the preparation process, and the compatibility of electrodes and electrolytes.

5.5 Emerging applications in cosmetics and bio-composites

Doped biochar is increasingly being explored for innovative applications in cosmetics and bio-composites, leveraging its unique properties such as high surface area, porosity, and tunable surface chemistry (Figure S5). Carbon material has gained popularity in cosmetics due to its excellent adsorption properties, making it a key ingredient in masks, cleansers, and soaps (Sajjad et al. 2021). Doping biochar with specific elements, such as iron or zinc, enhances its physicochemical properties, expanding its potential in skincare. For instance, zinc-doped biochar effectively adsorbs oils, dirt, and residues from the skin's surface (Masuku et al. 2024). It also removes heavy metals and organic pollutants from water used in cosmetics, ensuring safer and purer skincare products (Zhou et al. 2017). Additionally, zinc inhibits tyrosinase activity, reducing melanin production, which makes zinc-doped biochar a promising ingredient in whitening serums and blemish creams for improving skin tone and reducing pigmentation (Jeon et al. 2022). Beyond zinc, selenium-doped biochar offers strong antioxidant properties, beneficial in anti-aging creams, while silver-doped biochar provides antimicrobial and anti-inflammatory effects, making it ideal for acne treatments and soothing irritated skin (Sami et al. 2023; Feng et al. 2023). Despite these promising applications, research on element-doped biochar in cosmetics is still evolving. Further studies are needed to ensure its safety, stability, and efficacy in practical formulations.

Element-doped biochar has emerged as a transformative component in advanced bio-composites, leveraging tailored surface chemistry and structural modifications to enhance multifunctional performance. For instance, in bioplastics, the introduction of N-doped biochar significantly improves interfacial compatibility by forming strong chemical bonds (e.g., hydrogen bonds or van der Waals forces) with the polymer matrix, enhancing mechanical strength and durability (Ruan et al. 2025). Additionally, the porous structure of biochar increases internal friction within the material, impedes the slippage of molecular chains, and enhances stress transfer, thereby improving overall material strength (Sun et al. 2021). The functionalization of biochar through element doping also imparts unique properties to bio-composites. For example, silver-doped biochar confers antimicrobial properties, making it highly suitable for applications in food packaging and medical devices, where preventing microbial contamination is critical (Siddiqui et al. 2017). Similarly, the incorporation of conductive elements, such as copper/ceria-doped biochar, reduces surface resistance in functional coatings, providing excellent anti-static properties that protect electronic equipment from static damage (Melnik et al. 2009). In addition to these functionalities, certain dopants enhance the flame retardancy of coatings. When exposed to high temperatures, these elements form a dense carbonized layer that fills microscopic pores, isolating oxygen and heat. This mechanism improves flame resistance and reduces susceptibility to corrosion, making such coatings ideal for construction, furniture, and other applications requiring fire and corrosion safety (Cai et al. 2017; Yang et al. 2024a, b). Beyond traditional applications, doped biochar is also making strides in energy storage. For example, Chen et al. reported the use of N- and P-doped porous carbon nanosheets as a separator coating for high-energy-density Zn-I batteries. This material demonstrated exceptional electrochemical performance, with an initial capacity of 7.8 m Ah cm^{-2} at 20 mA cm^{-2} and an initial specific capacity of 8.9 m Ah cm^{-2} under high iodine loading. It also exhibited a retention rate of 56% (5.1 m Ah cm^{-2}) after 174 cycles, highlighting its potential for advanced energy storage systems (Chen et al. 2024). However, challenges persist in balancing dopant leaching resistance with biodegradability, necessitating atomic-level engineering of dopant–carbon bonding configurations.

6 Conclusion

This comprehensive review highlights the transformative potential of element-doped biochar as a versatile and sustainable material with exceptional physical and chemical properties. By systematically exploring innovative preparation methods, such as in-situ and exogenous doping, we have demonstrated how doping enhances the adsorption capacity, catalytic efficiency, and electrochemical performance of biochar. The integration of multiple elements into biochar not only optimizes its functionality but also expands its applications in environmental remediation, soil enhancement, energy conversion, and even cosmetics. The proposed

"preparation–structure–performance–application" framework provides a holistic approach to understanding and optimizing doped biochar, emphasizing the critical role of doping strategies and element selection in tailoring its properties for specific uses. Beyond consolidating existing knowledge, this review offers novel insights into emerging applications, such as carbon sequestration, pollutant adsorption, and advanced catalysis, while identifying future research directions to unlock the full potential of doped biochar. As the demand for sustainable materials grows, element-doped biochar stands out as a promising solution to addressing global challenges in environmental and energy sectors. This review not only advances the scientific understanding of doped biochar but also paves the way for its broader adoption, driving transformative progress in sustainable materials science and beyond.

7 Future prospect

Based on a comprehensive review of articles from 2018 to 2024 on Web of Science and X-mol academic platform using the keywords "biochar" and "doping", the number of relevant publications has shown a steady annual increase, as illustrated in Figure S6. This review highlights the significant contributions of element-doped biochar to environmental science, particularly in synthesis methods and performance optimization. However, existing doping techniques remain relatively simplistic, with challenges in precisely controlling the type and concentration of dopants. To advance this field, future research should focus on developing more efficient, stable, and environmentally friendly doping methods, optimizing multi-element doping structures, and exploring synergistic mechanisms and applications. Several key challenges must be addressed to advance the development and application of element-doped biochar:

- **Self-doping limitations:** Certain biowastes, such as crustacean shells (rich in Ca), animal viscera (rich in Fe), and aquatic plants (rich in N), enable self-doping. However, self-doping lacks precise control over element quantification and structural changes, and the underlying mechanisms remain unclear.
- **Interaction mechanisms:** The interaction between the carbon skeleton and doping elements during pyrolysis is poorly understood, posing potential risks for applications. Further research is needed to investigate doping ratios, element types, and their influence on the carbon structure.
- **Environmental concerns:** Some dopants, such as hydrochloric acid, phosphoric acid, and hydrofluoric acid, may cause secondary environmental contamination. Developing greener and eco-friendly dopants is crucial for sustainable progress.
- **Soil applications:** The extensive use of element-doped biochar may lead to soil nutrient imbalances and negatively impact microbial communities. Additionally, polycyclic aromatic hydrocarbons (PAHs) produced during pyrolysis can degrade soil quality. More in-depth studies are needed to assess its long-term effects on soil environments.
- **Doping efficiency and stability:** The effectiveness of heteroatom doping varies across applications, and the stability of dopants can fluctuate depending on environmental conditions. Achieving high doping efficiency and uniform distribution of heteroatoms on biochar surfaces remains a challenge.
- **Greenhouse gas emissions:** Pyrolysis for producing doped biochar inevitably generates greenhouse gases and potentially harmful byproducts. Careful selection of elements and optimization of preparation processes are essential to minimize environmental impacts.
- **Scalability challenges:** The industrial scalability of doped biochar depends on balancing cost-effectiveness, energy efficiency, and technological feasibility. High-purity dopants and energy-intensive methods currently limit large-scale applications. Future efforts should focus on expanding raw material sources, optimizing doping methods, leveraging existing infrastructure, and seeking government and industry support.

In summary, this review underscores the transformative potential of element-doped biochar in addressing global challenges such as pollution, soil degradation, and climate change. By adopting innovative doping techniques and a holistic framework, this study provides actionable insights for optimizing the performance of biochar in diverse applications, from environmental remediation to energy storage. It also serves as a comprehensive resource for researchers, promoting sustainable practices across industries and benefiting both the scientific community and society at large.

Supplementary Information

The online version contains supplementary material available at https://doi.org/10.1007/s42773-025-00467-x.

Additional file 1.

Author contributions

Junqi Zhao: Conceptualization, Writing-original draft. Yunqiu Jiang: Data curation, Methodology. Xinyu Chen: Data curation. Chongqing Wang: Writing-review & editing, Supervision. Hongyan Nan: Writing-review & editing, Funding acquisition.

Funding
This work is supported by National Natural Science Foundation of China (No. 42307312) and the China Postdoctoral Science Foundation (No. 2023M733218).

Availability of data and materials
Data will be made available on request.

Declarations

Competing interests
The authors have no relevant financial or non-financial interests to disclose.

Author details
[1]School of Chemical Engineering, Zhengzhou University, Zhengzhou 450001, China. [2]Hydrology and Water Resources Survey Bureau of the Upper Reaches of the Yangtze River, Hydrology Bureau of Yangtze River Water Resources Commission, Chongqing 400010, China.

Received: 19 December 2024 Revised: 6 April 2025 Accepted: 14 April 2025
Published online: 03 June 2025

References

Ahmad S, Liu L, Zhang S, Tang J (2023) Nitrogen-doped Biochar (N-doped BC) and Iron/Nitrogen Co-doped Biochar (Fe/N co-doped BC) for removal of refractory organic pollutants. J Hazard Mater 446:130727. https://doi.org/10.1016/j.jhazmat.2023.130727

Ahmad S, Liu X, Liu L, Waqas M, Zhang J, Hassan MA, Zhang S, Pan B, Tang J (2024) Remediation of chromium contaminated water and soil by nitrogen and iron doped biochars. Sci Total Environ 954:176435. https://doi.org/10.1016/j.scitotenv.2024.176435

Alhashimi HA, Aktas CB (2017) Life cycle environmental and economic performance of biochar compared with activated carbon: a meta-analysis. Resour Conserv Recycl 118:13–26. https://doi.org/10.1016/j.resconrec.2016.11.016

Aller MF (2016) Biochar properties: transport, fate, and impact. Crit Rev Environ Sci Technol 46(14–15):1183–1296. https://doi.org/10.1080/10643389.2016.1212368

Ambursa M, Juan J, Yahaya Y, Taufiq-Yap Y, Lin Y, Lee H (2020) A review on catalytic hydrodeoxygenation of lignin to transportation fuels by using nickel-based catalysts. Renew Sustain Energy Rev 138:110667. https://doi.org/10.1016/j.rser.2020.110667

Anum S, Liu S, Zhang P, Bostani A, Wang X, Sun H (2024) Sand-milled nano-sized N-doped biochar for the efficient remediation of Pb- and Cd-contaminated soil: Preparation, performance and mechanism. J Environ Chem Eng 12(5):114007. https://doi.org/10.1016/j.jece.2024.114007

Aziz S, Uzair B, Ali MI, Anbreen S, Umber F, Khalid M, Aljabali AA, Mishra Y, Mishra V, Serrano-Aroca Á, Naikoo GA, El-Tanani M, Haque S, Almutary AG, Tambuwala MM (2023) Synthesis and characterization of nanobiochar from rice husk biochar for the removal of safranin and malachite green from water. Environ Res 238:116909. https://doi.org/10.1016/j.envres.2023.116909

Bai Y, Shi C, Ma X, Li J, Chen S, Guo N, Yu X, Yang C, Zhang Z (2022) Encapsulation of Zn/Co nanocrystals into sponge-like 3D porous carbon for Escherichia coli inactivation coupled with ultrasound: characterization, kinetics and inactivation mechanism. Chem Eng J 447:137545. https://doi.org/10.1016/j.cej.2022.137545

Biswas B, Adhikari S, Jahromi H, Ammar M, Baltrusaitis J, Torbert A, Linhoss J, Lamba J (2024) Magnesium doped biochar for simultaneous adsorption of phosphate and nitrogen ions from aqueous solution. Chemosphere 358:142130. https://doi.org/10.1016/j.chemosphere.2024.142130

Cai W, Wang J, Quan X, Zhao S, Wang Z (2017) Antifouling and anticorrosion properties of one-pot synthesized dedoped bromo-substituted polyaniline and its composite coatings. Surf Coat Technol 334:7–18. https://doi.org/10.1016/j.surfcoat.2017.10.076

Carneiro JS, Lustosa Filho JF, Nardis BO, Ribeiro-Soares J, Zinn YL, Melo LC (2018) Carbon stability of engineered biochar-based phosphate fertilizers. ACS Sustain Chem Eng 6(11):14203–14212. https://doi.org/10.1021/acssuschemeng.8b02841

Caron A, Ali I, Delgado M, Johnson D, Reeks J, Strzhemechny Y, McGillivray S (2024) Zinc oxide nanoparticles mediate bacterial toxicity in Mueller-Hinton Broth via Zn^{2+}. Front Microbiol 15:1394078. https://doi.org/10.3389/fmicb.2024.1394078

Chacón FJ, Sánchez-Monedero MA, Lezama L, Cayuela ML (2020) Enhancing biochar redox properties through feedstock selection, metal preloading and post-pyrolysis treatments. Chem Eng J 395:125100. https://doi.org/10.1016/j.cej.2020.125100

Chaturvedi K, Singhwane A, Dhangar M, Mili M, Gorhae N, Naik A, Prashant N, Srivastava AK, Verma S (2023) Bamboo for producing charcoal and biochar for versatile applications. Biomass Conversion and Biorefinery 14(15):177041–217053. https://doi.org/10.1007/s13399-022-03715-3

Chen AB, Yu YF, Zang WW, Qi GL, Yu YH, Li YT (2015) Nitrogen-doped porous carbon for CO_2 adsorption. J Inorg Mater 30(1):9–16. https://doi.org/10.1554/jim20140175

Chen J, Chen D, Xu Q, Fuhrmann JJ, Li L, Pan G, Li Y, Qin H, Liang C, Sun X (2018) Organic carbon quality, composition of main microbial groups, enzyme activities, and temperature sensitivity of soil respiration of an acid paddy soil treated with biochar. Biol Fertil Soils 55(2):185–197. https://doi.org/10.1007/s00374-018-1333-2

Chen W, Meng J, Han X, Lan Y, Zhang W (2019) Past, present, and future of biochar. Biochar 1(1):75–87. https://doi.org/10.1007/s42773-019-00008-3

Chen W, Fang Y, Li K, Chen Z, Xia M, Gong M, Chen Y, Yang H, Tu X, Chen H (2020) Bamboo wastes catalytic pyrolysis with N-doped biochar catalyst for phenols products. Appl Energy 260:114242. https://doi.org/10.1016/j.apenergy.2019.114242

Chen W, Lei L, Zhu K, He D, He H, Li X, Wang Y, Huang J, Ai Y (2022) Peroxymonosulfate activation by Fe-N-S co-doped tremella-like carbocatalyst for degradation of bisphenol A: synergistic effect of pyridine N, Fe-Nx, thiophene S. J Environ Sci 129:213–228. https://doi.org/10.1016/j.jes.2022.09.037

Chen Q, Cheng X, Liu S, Xia D, Liu Y, Zhang Z, Gu P (2023) Multi-heteroatom self-doped microporous biochar derived from fish scale for boosting uranium immobilization performance. Diamond Relat Mater 136:110052. https://doi.org/10.1016/j.diamond.2023.110052

Chen S, Tian L, Feng X, Bao H, Wang H (2024) Biomaterial-derived porous carbon doped with heteroatoms as a separator coating for high-energy–density Zn-I batteries. Biochar 6(1):99. https://doi.org/10.1007/s42773-024-00399-y

Cheng T, Bian Y, Li J, Ma X, Yang L, Zhou L, Wu H (2022) Nitrogen-doped porous biochar for selective adsorption of toluene under humid conditions. Fuel 334:126452. https://doi.org/10.1016/j.fuel.2022.126452

Cheng Y, Yang J, Shen J, Yan P, Liu S, Kang J, Bi L, Wang B, Zhao S, Chen Z (2023) Preparation of P-doped biochar and its high-efficient removal of sulfamethoxazole from water: Adsorption mechanism, fixed-bed column and DFT study. Chem Eng J 468:143748. https://doi.org/10.1016/j.cej.2023.143748

Cho S, Hyun JC, Ha S, Choi Y, Seong H, Choi J, Jin HJ, Yun YS (2022) Sulfur-doped hard carbon hybrid anodes with dual lithium-ion/metal storage bifunctionality for high-energy-density lithium-ion batteries. Carbon Energy 5(1):288. https://doi.org/10.1002/cey2.288

Da Y, Xu M, Ma J, Gao P, Zhang X, Yang G, Wu J, Song C, Long L, Chen C (2023) Remediation of cadmium contaminated soil using K_2FeO_4 modified vinasse biochar. Ecotoxicol Environ Saf 262:115171. https://doi.org/10.1016/j.ecoenv.2023.115171

Deng J, Li J, Song S, Zhou Y, Li L (2020) Electrolyte-dependent supercapacitor performance on nitrogen-doped porous bio-carbon from gelatin. Nanomaterials 10(2):353. https://doi.org/10.3390/nano10020353

Deng L, Jin X, Zhang K, Jiang J, Zhu Z, Che D (2022) Catalytic conversion of toluene by modified biochar from oak. J Energy Inst 102:374–383. https://doi.org/10.1016/j.joei.2022.05.002

Ding D, Yang S, Qian X, Chen L, Cai T (2020) Nitrogen-doping positively whilst sulfur-doping negatively affect the catalytic activity of biochar for the degradation of organic contaminant. Appl Catal b: Environ 263:118348. https://doi.org/10.1016/j.apcatb.2019.118348

Dinh VC, Hou C-H, Dao TN (2022) O, N-doped porous biochar by air oxidation for enhancing heavy metal removal: the role of O N functional groups. Chemosphere 293:133622. https://doi.org/10.1016/j.chemosphere.2022.133622

Fan M, Li C, Sun Y, Zhang L, Zhang S, Hu X (2021) In situ characterization of functional groups of biochar in pyrolysis of cellulose. Sci Total Environ 799:149354. https://doi.org/10.1016/j.scitotenv.2021.149354

Feng Q, Fan B, He Y-C, Ma C (2023) Antibacterial, antioxidant and fruit packaging ability of biochar-based silver nanoparticles-polyvinyl alcohol-chitosan composite film. Int J Biol Macromol 256:128297. https://doi.org/10.1016/j.ijbiomac.2023.128297

Feng X, Ma X, Niu C, Zhang R, Yang X, Ma H, Li W, Li S (2024a) N self-doping hierarchical porous biochar from Chinese medicine residues for efficient removal of malachite green: Critical contribution of N doping to *π-π* electron donor-donor interactions. Ind Crops Prod 221:119367. https://doi.org/10.1016/j.indcrop.2024.119367

Feng Y, Wu X, Hong N, Zhang L, Zhang X, Liu Y, Zheng H, Zhang Q, Ruan R, Cobb K (2024b) Nitrogen-doped biochar from algal biomass: preparation, modification, and application. Biomass Conv Bioref 14(23):29221–29234. https://doi.org/10.1007/s13399-023-04942-y

Fu Q, Sun S, Li N, Lu K, Dong Z (2023a) Based on halogen-doped carbon dots: a review. Mater Today Chem 34:101769. https://doi.org/10.1016/j.mtchem.2023.101769

Fu S, Li M, de Jong W, Kortlever R (2023b) Tuning the properties of N-doped biochar for selective CO2 electroreduction to CO. ACS Catal 13(15):10309–10323. https://doi.org/10.1021/acscatal.3c01773

Gao R, Wang Q, Liu Y, Zhu J, Deng Y, Fu Q, Hu H (2018) Co-pyrolysis biochar derived from rape straw and phosphate rock: carbon retention, aromaticity, and pb removal capacity. Energy Fuels 33(1):413–419. https://doi.org/10.1021/acs.energyfuels.8b03753

Gao W, Lin Z, Chen H, Yan S, Zhu H, Zhang H, Sun H, Zhang S, Zhang S, Wu Y (2022) Roles of graphitization degree and surface functional groups of N-doped activated biochar for phenol adsorption. J Anal Appl Pyrol 167:105700. https://doi.org/10.1016/j.jaap.2022.105700

Gao Y, Sun Y, Song W, Jia Y, Li A, Wang S (2023a) Intrinsic properties of biochar for electron transfer. Chem Eng J 475:146356. https://doi.org/10.1016/j.cej.2023.146356

Gao X, Zhang H, Zhang J, Weng N, Huo S (2023b) Inactivation of harmful cyanobacteria Microcystis aeruginosa by Cu^{2+} doped corn stalk biochar treated with different pyrolysis temperatures. Biores Technol 394:130259. https://doi.org/10.1016/j.biortech.2023.130259

Geng Y, Wang J, Wang Q, Chen X, Sun S, Zhang S, Tian Y, Liu C, Wang L, Wei Z, Cao L, Zhang J, Zhang S (2023) N/O Co-doped hierarchical nanoporous biochar derived from waste polypropylene nonwoven for high-performance supercapacitors. RSC Adv 13(37):25877–25887. https://doi.org/10.1039/d3ra04862d

Gopalakrishnan A, Badhulika S (2020) Effect of self-doped heteroatoms on the performance of biomass-derived carbon for supercapacitor applications. J Power Sour 480:228830. https://doi.org/10.1016/j.jpowsour.2020.228830

Guo R, Yan L, Rao P, Wang R, Guo X (2020a) Nitrogen and sulfur co-doped biochar derived from peanut shell with enhanced adsorption capacity for diethyl phthalate. Environ Pollut 258:113674. https://doi.org/10.1016/j.envpol.2019.113674

Guo Y, Tan C, Sun J, Li W, Zhang J, Zhao C (2020b) Biomass ash stabilized MgO adsorbents for CO_2 capture application. Fuel 259:116298. https://doi.org/10.1016/j.fuel.2019.116298

Guo L, Zhao L, Tang Y, Zhou J, Shi B (2023) Peroxydisulfate activation using Fe Co co-doped biochar and synergistic effects on tetracycline degradation. Chem Eng J 452:139381. https://doi.org/10.1016/j.cej.2022.139381

Haoming C, Lingyi T, Yishu H, Yuanyuan G, Lingzi M, Weinan L, Zhijun W, Zhen L, Zongli H (2022) Investigating the pathways of enhanced Pb immobilization by chlorine-loaded biochar. J Clean Prod 344:131097. https://doi.org/10.1016/j.jclepro.2022.131097

Hassaan MA, Elkatory MR, El-Nemr MA, Ragab S, Yi X, Huang M, El Nemr A (2024) Synthesis, characterization, optimization and application of Pisum sativum peels S and N-doping biochars in the production of biogas from Ulva lactuca. Renew Energy 221:119747. https://doi.org/10.1016/j.renene.2023.119747

He Y, Chen S, Chen J, Liu D, Ning X, Liu J, Wang T (2019) Consequence of replacing nitrogen with carbon dioxide as atmosphere on suppressing the formation of polycyclic aromatic hydrocarbons in catalytic pyrolysis of sawdust. Biores Technol 297:122417. https://doi.org/10.1016/j.biortech.2019.122417

Hu X, Ding Z, Zimmerman AR, Wang S, Gao B (2014) Batch and column sorption of arsenic onto iron-impregnated biochar synthesized through hydrolysis. Water Res 68:206–216. https://doi.org/10.1016/j.watres.2014.10.009

Hu S, Liu C, Bu H, Chen M, Tang J, Jiang B, Ran Y (2024) Reduced sulfur compounds and carboxylic acid groups in dissolved PFRs of iron-biochar enhance Cr(VI) reduction in anaerobic conditions. Biochar 6(1):13. https://doi.org/10.1007/s42773-024-00305-6

Huang D, Zhang Q, Zhang C, Wang R, Deng R, Luo H, Li T, Li J, Chen S, Liu C (2020) Mn doped magnetic biochar as persulfate activator for the degradation of tetracycline. Chem Eng J 391:123532. https://doi.org/10.1016/j.cej.2019.123532

Huang K, Chang M, Zhang J, Luo Z, Zhang Y, Zhao K, Wang W, Chen D (2023a) Exploring the impact of ni doping on bagasse biochar and its efficient hydrogen production via assisted water electrolysis. Energ Technol 11(7):2201450. https://doi.org/10.1002/ente.202201450

Huang P, Zhang P, Wang C, Du X, Jia H, Sun H (2023b) P-doped biochar regulates nZVI nanocracks formation for superefficient persulfate activation. J Hazard Mater 450:130999. https://doi.org/10.1016/j.jhazmat.2023.130999

Hung CM, Chen CW, Huang CP, Yang YY, Dong CD (2022) Suppression of polycyclic aromatic hydrocarbon formation during pyrolytic production of lignin-based biochar via nitrogen and boron co-doping. Biores Technol 355:127246. https://doi.org/10.1016/j.biortech.2022.127246

Jannis G, Dilani R, Nikolas H, Thomas DB, Hans-Peter S (2024) Biochars from chlorine-rich feedstock are low in polychlorinated dioxins, furans and biphenyls. J Anal Appl Pyrol 183:106764. https://doi.org/10.1016/j.jaap.2024.106764

Jeon G, Choi H, Park D-J, Nguyen N-T, Kim Y-H, Min J (2022) Melanin treatment effect of vacuoles-zinc oxide nanoparticles combined with ascorbic acid. Mol Biotechnol 65(7):1119–1128. https://doi.org/10.1007/s12033-022-00608-8

Jia L, Fan B-G, Yao Y-X, Han F, Huo R-P, Zhao C-W, Jin Y (2018) Study on the elemental mercury adsorption characteristics and mechanism of iron-based modified biochar materials. Energy Fuels 32(12):12554–12566. https://doi.org/10.1021/acs.energyfuels.8b02890

Jia L, Yu Y, Li ZP, Qin SN, Guo JR, Zhang YQ, Wang JC, Zhang JC, Fan BG, Jin Y (2021) Study on the Hg0 removal characteristics and synergistic mechanism of iron-based modified biochar doped with multiple metals. Biores Technol 332:125086. https://doi.org/10.1016/j.biortech.2021.125086

Jin Z, Li Y, Dong H, Xiao S, Xiao J, Chu D, Hou X, Xiang S, Dong Q, Li L (2022) A comparative study on the activation of persulfate by mackinawite@biochar and pyrite@biochar for sulfamethazine degradation: the role of different natural iron-sulfur minerals doping. Chem Eng J 448:137620. https://doi.org/10.1016/j.cej.2022.137620

Jing S, Ding P, Zhang Y, Liang H, Yin S, Tsiakaras P (2019) Lithium-sulfur battery cathodes made of porous biochar support CoFe@NC metal nanoparticles derived from Prussian blue analogues. Ionics 25(11):5297–5304. https://doi.org/10.1007/s11581-019-03065-7

Ju W, Xu X, Chen H, Xu X, Ma Z, Wang X, Lei W (2023) Nitrogen-doped porous biochar spheres/Mn3O4 heterostructure as an efficient sulfur host for high performance lithium-sulfur batteries. Mater Res Bull 167:112410. https://doi.org/10.1016/j.materresbull.2023.112410

Kang B, Chen X, Zeng L, Luo F, Li X, Xu L, Yang M-Q, Chen Q, Wei M, Qian Q (2020) In situ fabrication of ultrathin few-layered WSe anchored on N, P dual-doped carbon by bioreactor for halffull sodiumpotassium-ion batteries with ultralong cycling lifespan. J Colloid Interface Sci 574:217–228. https://doi.org/10.1016/j.jcis.2020.04.055

Kang B, Wang Y, He X, Wu Y, Li X, Lin C, Chen Q, Zeng L, Wei M, Qian Q (2021) Facile fabrication of WS_2 nanocrystals confined in chlorella-derived N, P co-doped bio-carbon for sodium-ion batteries with ultra-long lifespan. Dalton Trans 50(41):14745–14752. https://doi.org/10.1039/d1dt01582f

Kim DK, Jo DY, Yu J, Park S-K, Yoo Y (2024) In-situ doped and activated N, S co-doped porous carbon derived from organic salt for application in high-performance potassium-ion batteries. J Energy Storage 100:113380. https://doi.org/10.1016/j.est.2024.113380

Kong G, Liu Q, Ji G, Jia H, Cao T, Zhang X, Han L (2023) Improving hydrogen-rich gas production from biomass catalytic steam gasification over metal-doping porous biochar. Biores Technol 387:129662. https://doi.org/10.1016/j.biortech.2023.129662

Lavine MS (2018) The twisted carbon nanotube story. Science 362(6411):194–195. https://doi.org/10.1126/science.362.6411.194-h

Leng L, Xu X, Wei L, Fan L, Huang H, Li J, Lu Q, Li J, Zhou W (2019) Biochar stability assessment by incubation and modelling: Methods, drawbacks and recommendations. Sci Total Environ 664:11–23. https://doi.org/10.1016/j.scitotenv.2019.01.298

Leng L, Liu R, Xu S, Mohamed BA, Yang Z, Hu Y, Chen J, Zhao S, Wu Z, Peng H, Li H, Li H (2022) An overview of sulfur-functional groups in biochar from pyrolysis of biomass. J Environ Chem Eng 10(2):107185. https://doi.org/10.1016/j.jece.2022.107185

Li H, Dong X, da Silva EB, de Oliveira LM, Chen Y, Ma LQ (2017a) Mechanisms of metal sorption by biochars: biochar characteristics and modifications. Chemosphere 178:466–478. https://doi.org/10.1016/j.chemosphere.2017.03.072

Li Q, Guo X, Zhang Y, Zhang W, Ge C, Zhao L, Wang X, Zhang H, Chen J, Wang Z, Sun L (2017b) Porous graphene paper for supercapacitor applications. J Mater Sci Technol 33(8):793–799. https://doi.org/10.1016/j.jmst.2017.03.018

Li P, Li Z, Cui J, Geng C, Kang Y, Zhang C, Yang C (2019) N-doped graphene/$CoFe_2O_4$ catalysts for the selective catalytic reduction of NO_x by NH_3. RSC Adv 9(28):15791–15797. https://doi.org/10.1039/c9ra02456e

Li X, Jia Y, Zhou M, Su X, Sun J (2020) High-efficiency degradation of organic pollutants with Fe, N co-doped biochar catalysts via persulfate activation. J Hazard Mater 397:122764. https://doi.org/10.1016/j.jhazmat.2020.122764

Li H, Mingjun L, Feng Z, Jing W, Lai C, Pengfei H, Qiang Z, Sajid B, Jingbo Louise L (2021a) Efficient removal of water pollutants by hierarchical porous zeolite-activated carbon prepared from coal gangue and bamboo. J Clean Prod 325:129322. https://doi.org/10.1016/j.jclepro.2021.129322

Li S, Ma X, Ma Z, Dong X, Wei Z, Liu X, Zhu L (2021b) Mg/Al-layered double hydroxide modified biochar for simultaneous removal phosphate and nitrate from aqueous solution. Environ Technol Innov 23:101771. https://doi.org/10.1016/j.eti.2021.101771

Li H, Jiang Q, Li R, Zhang B, Zhang J, Zhang Y (2022a) Passivation of lead and cerium in soil facilitated by biochar-supported phosphate-doped ferrihydrite: mechanisms and microbial community evolution. J Hazard Mater 436:129090. https://doi.org/10.1016/j.jhazmat.2022.129090

Li D, Wen C, Huang J, Zhong J, Chen P, Liu H, Wang Z, Liu Y, Lv W, Liu G (2022b) High-efficiency ultrathin porous phosphorus-doped graphitic carbon nitride nanosheet photocatalyst for energy production and environmental remediation. Appl Catal B-Environ Energy 307:121099. https://doi.org/10.1016/j.apcatb.2022.121099

Li S, Wen Y, Wang Y, Liu M, Su L, Peng Z, Zhou Z, Zhou N (2023a) Novel α-amino acid-like structure decorated biochar for heavy metal remediation in acid soil. J Hazard Mater 462:132740. https://doi.org/10.1016/j.jhazmat.2023.132740

Li X, Zeng J, Zuo S, Lin S, Chen G (2023b) Preparation, modification, and application of biochar in the printing field: a review. Materials 16(14):5081. https://doi.org/10.3390/ma16145081

Li F, Wang X, Xu C (2023c) Research progress on structural characteristics, structure-application relationships, and environmental application of biochar-supported zero valent iron (ZVI-BC). Curr Pollut Rep 9(2):292–311. https://doi.org/10.1007/s40726-023-00260-z

Liang X, Guo N, Zhao Y, Xue F, Ren X, Yang Z, Yang Q (2022) Rapid effectual entrapment of pesticide pollutant by phosphorus-doped biochar: Effects and response sequence of functional groups. J Mol Liq 365:120155. https://doi.org/10.1016/j.molliq.2022.120155

Liao H, Fan S, Han W, Wang M, Shi Q, Xie Y, Yang X, Chen W (2024) Machine learning prediction of supercapacitor performance of N-doped biochar from biomass wastes based on N-containing groups, element compositions, and pore structures. J Energy Stor 100:113548. https://doi.org/10.1016/j.est.2024.113548

Lin M, Li F, Li X, Rong X, Oh K (2023a) Biochar-clay, biochar-microorganism and biochar-enzyme composites for environmental remediation: a review. Environ Chem Lett 21(3):1837–1862. https://doi.org/10.1007/s10311-023-01582-6

Lin C, Xia J, Shenggui M, Wenhua C, Bo X, Zhongde D, Wenju J, Yue P, Junhua L (2023b) Towards highly exposed active sites via Edge-N-rich carbon nanosheet @ porous biochar for efficient H_2S catalytic oxidation. Chem Eng J 475:146115. https://doi.org/10.1016/j.cej.2023.146115

Lina L, Xuehui S, Cong N, Mantang C, Yipeng W, Qingzhu Z, Yang X (2024) Salts-activated synthesis of Cu/Co co-doped biochar for efficient removal of elemental mercury from coal combustion flue gas. Chem Eng J 499:156174. https://doi.org/10.1016/j.cej.2024.156174

Ling L, Liu W, Zhang S, Jiang H (2017) Magnesium oxide embedded nitrogen self-doped biochar composites: fast and high-efficiency adsorption of heavy metals in an aqueous solution. Environ Sci Technol 51(17):10081–10089. https://doi.org/10.1021/acs.est.7b02382

Liu WJ, Li WW, Jiang H, Yu HQ (2017a) Fates of chemical elements in biomass during its pyrolysis. Chem Rev 117(9):6367–6398. https://doi.org/10.1021/acs.chemrev.6b00647

Liu Y, Yao S, Wang Y, Lu H, Brar SK, Yang S (2017b) Bio- and hydrochars from rice straw and pig manure: Inter-comparison. Biores Technol 235:332–337. https://doi.org/10.1016/j.biortech.2017.03.103

Liu L, Niu Z, Chen J (2018) Flexible supercapacitors based on carbon nanotubes. Chin Chem Lett 13(7):1825–1841. https://doi.org/10.1016/j.cclet.2018.01.013

Liu J, Kang X, He X, Wei P, Wen Y, Li X (2019) Temperature-directed synthesis of N-doped carbon-based nanotubes and nanosheets decorated with Fe (Fe_3O_4, Fe_3C) nanomaterials†. Nanoscale 11(18):9155–9162. https://doi.org/10.1039/c9nr01601e

Liu B, Guo W, Wang H, Si Q, Zhao Q, Luo H, Ren N (2020a) B-doped graphitic porous biochar with enhanced surface affinity and electron transfer for efficient peroxydisulfate activation. Chem Eng J 396:125119. https://doi.org/10.1016/j.cej.2020.125119

Liu Y, Gao C, Wang Y, He L, Lu H, Yang S (2020b) Vermiculite modification increases carbon retention and stability of rice straw biochar at different carbonization temperatures. J Clean Prod 254:120111. https://doi.org/10.1016/j.jclepro.2020.120111

Liu Y, Chen Y, Li Y, Chen L, Jiang H, Li H, Luo X, Tang P, Yan H, Zhao M, Yuan Y, Hou S (2022) Fabrication, application, and mechanism of metal and heteroatom co-doped biochar composites (MHBCs) for the removal of contaminants in water: a review. J Hazard Mater 431:128584. https://doi.org/10.1016/j.jhazmat.2022.128584

Liu Z, Chen R, Li M, Yang S, Zhang J, Yuan S, Hou Y, Li C, Chen Y (2023) Manganese-nitrogen co-doped biochar (MnN@BC) as particle electrode for three-dimensional (3D) electro-activation of peroxydisulfate: active sites enhanced radical/non-radical oxidation. J Hazard Mater 459:132089. https://doi.org/10.1016/j.jhazmat.2023.132089

Liu T, Shao T, Jiang J, Ma W, Feng R, Dong D, Wang Y, Bai T, Xu Y (2024) Influence of potassium addition on phosphorus availability and heavy metals immobility of biochar derived from swine manure. Sci Rep 14:21069. https://doi.org/10.1038/s41598-024-69761-1

Lu X, Wang J, Peng W, Li N, Liang L, Cheng Z, Yan B, Yang G, Chen G (2023) Electrocatalytic hydrogenation of phenol by active sites on Pt-decorated shrimp shell biochar catalysts: Performance and internal mechanism. Fuel 331:125845. https://doi.org/10.1016/j.fuel.2022.125845

Luo K, Wen Y, Kang X (2022) Halogen-doped carbon dots: synthesis, application, and prospects. Molecules 27(14):4620. https://doi.org/10.3390/molecules27144620

Luo J, Chen Y, Huang H, Ma R, Ma N, Yan F, Xu J, Zhang J, Chen J, Sun S (2023) Microwave-coordinated KOH directionally modulated N/O co-doped porous biochar from enteromorpha and its structure–effect relationships in efficient CO_2 capture. Chem Eng J 473:145279. https://doi.org/10.1016/j.cej.2023.145279

Luo Q, Zeng T, Gu K, Lin Q, Yang W (2024) Research progress of lignin-derived functional materials for electrochemical energy storage. ACS Appl Energy Mater 7(24):11610–11632. https://doi.org/10.1021/acsaem.4c01294

Mahesan Naidu S, Zhentao W, Pei Sean G, Shouyong Z (2023) The state-of-the-art development of biochar based photocatalyst for removal of various organic pollutants in wastewater. J Clean Prod 429:139487. https://doi.org/10.1016/j.jclepro.2023.139487

Makinde WO, Hassan MA, Pan Y, Guan G, López-Salas N, Khalil ASG (2024) Sulfur and nitrogen co-doping of peanut shell-derived biochar for sustainable supercapacitor applications. J Alloy Compd 991:174452. https://doi.org/10.1016/j.jallcom.2024.174452

Malavekar DB, Magdum VV, Khot SD, Kim JH, Lokhande CD (2023) Doping of rare earth elements: towards enhancing the electrochemical performance of pseudocapacitive materials. J Alloy Compd 960:176602. https://doi.org/10.1016/j.jallcom.2023.170601

Manickavasagam G, He C, Lin K-YA, Saaid M, Oh WD (2024) Recent advances in catalyst design, performance, and challenges of metal-heteroatom-co-doped biochar as peroxymonosulfate activator for environmental remediation. Environ Res 252:118919. https://doi.org/10.1016/j.envres.2024.118919

Mašek O, Buss W, Brownsort P, Rovere M, Tagliaferro A, Zhao L, Cao X, Xu G (2019) Potassium doping increases biochar carbon sequestration potential by 45%, facilitating decoupling of carbon sequestration from soil improvement. Sci Rep 9(1):5514. https://doi.org/10.1038/s41598-019-41953-0

Masuku M, Nure JF, Atagana HI, Hlongwa N, Nkambule TTI (2024) Advancing the development of nanocomposite adsorbent through zinc-doped nickel ferrite-pinecone biochar for removal of chromium (VI) from wastewater. Sci Total Environ 908:168136. https://doi.org/10.1016/j.scitotenv.2023.168136

Matskevich NI, Semerikova AN, Samoshkin DA, Stankus SV, Zaitsev VP, Kuznetsov VA, Novikov AY (2023) Synthesis, thermodynamic properties, and ionic conductivity of compounds based on bismuth niobates doped by rare-earth elements (a review). Russ J Inorg Chem 68(11):1632–1649. https://doi.org/10.1134/s0036023623602179

Mayilswamy N, Nighojkar A, Edirisinghe M, Sundaram S, Kandasubramanian B (2023) Sludge-derived biochar: physicochemical characteristics for environmental remediation. Appl Phys Rev 10(3):031308. https://doi.org/10.1063/5.0137651

Melnik J, Fu XZ, Luo JL, Sanger AR, Chuang KT, Yang QM (2009) Ceria and copper/ceria functional coatings for electrochemical applications: materials preparation and characterization. J Power Sources 195(8):2189–2195. https://doi.org/10.1016/j.jpowsour.2009.10.076

Meng X-R, Gao S, Liu N, Wu P-D, Fang Z (2024) Regulating N-doped biochar with Fe-Mo heterojunctions as cathode in long-life zinc-air battery. Chem Eng J 500:157463. https://doi.org/10.1016/j.cej.2024.157463

Mian MM, Liu G, Yousaf B, Fu B, Ullah H, Ali MU, Abbas Q, Mujtaba Munir MA, Ruijia L (2018) Simultaneous functionalization and magnetization of biochar via NH_3 ambiance pyrolysis for efficient removal of Cr (VI). Chemosphere 208:712–721. https://doi.org/10.1016/j.chemosphere.2018.06.021

Mian MM, Liu G, Yousaf B, Fu B, Ahmed R, Abbas Q, Munir MAM, Ruijia L (2019) One-step synthesis of N-doped metal/biochar composite using NH_3-ambiance pyrolysis for efficient degradation and mineralization of Methylene Blue. J Environ Sci 78:29–41. https://doi.org/10.1016/j.jes.2018.06.014

Miao W, Liu W, Ding Y, Guo R, Zhao J, Zhu Y, Yu H, Zhu Y (2022) Cobalt (iron), nitrogen and carbon doped mushroom biochar for high-efficiency oxygen reduction in microbial fuel cell and Zn-air battery. J Environ Chemi Eng. 10(5):108474. https://doi.org/10.1016/j.jece.2022.108474

Moralı U, Yavuzel N, Şensöz S (2016) Pyrolysis of hornbeam (Carpinus betulus L.) sawdust: Characterization of bio-oil and bio-char. Biores Technol 221:682–685. https://doi.org/10.1016/j.biortech.2016.09.081

Mujtaba Munir MA, Yousaf B, Ali MU, Dan C, Abbas Q, Arif M, Yang X (2021) In situ synthesis of micro-plastics embedded sewage-sludge co-pyrolyzed biochar: implications for the remediation of Cr and Pb availability and enzymatic activities from the contaminated soil. J Clean Prod 302:127005. https://doi.org/10.1016/j.jclepro.2021.127005

Nan H, Zhao L, Yang F, Liu Y, Xiao Z, Cao X, Qiu H (2020) Different alkaline minerals interacted with biomass carbon during pyrolysis: Which one improved biochar carbon sequestration? J Clean Prod 255:120162. https://doi.org/10.1016/j.jclepro.2020.120162

Nguyen TB, Nguyen TKT, Chen CW, Chen WH, Bui XT, Lam SS, Dong CD (2023) $NiCo_2O_4$-loaded sunflower husk-derived biochar as efficient peroxymonosulfate activator for tetracycline removal in water. Biores Technol 382:129182. https://doi.org/10.1016/j.biortech.2023.129182

Nurgül Ö, Adife Şeyda Y, Elif Y, Rahmiye Zerrin Y, Kamil Burak D, Servet T (2023) Production of Si-doped biomass-derived materials: effect of support type, activation and doping conditions. Biomass Convers Bioref 14:31369–31381. https://doi.org/10.1007/s13399-023-04786-6

Oh WD, Zaeni JRJ, Lisak G, Lin KYA, Leong KH, Choong ZY (2021) Accelerated organics degradation by peroxymonosulfate activated with biochar co-doped with nitrogen and sulfur. Chemosphere 277:130313. https://doi.org/10.1016/j.chemosphere.2021.130313

Pamphile N, Hongwei R, Pancras N, Jean Pierre M, François N, Shiyi L, Dabin G, Baihui C (2023) A review on activated carbon/ graphene composite-based materials: synthesis and applications. J Clean Prod 417:138006. https://doi.org/10.1016/j.jclepro.2023.138006

Patel MA, Luo F, Khoshi MR, Rabie E, Zhang Q, Flach CR, Mendelsohn R, Garfunkel E, Szostak M, He H (2016) P-doped porous carbon as metal free catalysts for selective aerobic oxidation with an unexpected mechanism. ACS Nano 10(2):2305–2315. https://doi.org/10.1021/acsnano.5b07054

Pongpanyanate K, Roddecha S, Piyanirund C, Phraewphiphat T, Hasin P (2024) Dispersed MnO_2 nanoparticles/sugarcane bagasse-derived carbon composite as an anode material for lithium-ion batteries. RSC Adv 14:2354–2368. https://doi.org/10.1039/d3ra04008a

Qi H, Pan G, Shi X, Sun Z (2022) Cu–Fe–FeC_3@nitrogen-doped biochar microsphere catalyst derived from CuFe2O4@chitosan for the efficient removal of amoxicillin through the heterogeneous electro-Fenton process. Chem Eng J 434:134675. https://doi.org/10.1016/j.cej.2022.134675

Qi Y, Sun L, Liu Z (2024) Super graphene-skinned materials: an innovative strategy toward graphene applications. ACS Nano 18(6):4617–4623. https://doi.org/10.1021/acsnano.3c11971

Radosław K, Marcin F, Bogdan S (2024) Opportunities and threats for supercapacitor technology based on biochar-a review. Energies 17(18):4617. https://doi.org/10.3390/en17184617

Rajapaksha AU, Chen SS, Tsang DCW, Zhang M, Vithanage M, Mandal S, Gao B, Bolan NS, Ok YS (2016) Engineered/designer biochar for contaminant removal/immobilization from soil and water: Potential and implication of biochar modification. Chemosphere 148:276–291. https://doi.org/10.1016/j.chemosphere.2016.01.043

Rakesh K, Lakshmi Prasanna L, Rama Rao K, Zahid Husain M, Janardhan Reddy K, Yoon-Young C (2023) Catalytic efficiency of LDH@carbonaceous hybrid nanocomposites towards water splitting mechanism: Impact of plasma and its significance on HER and OER activity. Coord Chem Rev 497:215460. https://doi.org/10.1016/j.ccr.2023.215460

Ren N, Tang Y, Li M (2018) Mineral additive enhanced carbon retention and stabilization in sewage sludge-derived biochar. Process Saf Environ Prot 115:70–78. https://doi.org/10.1016/j.psep.2017.11.006

Resego P, Sanjay Mavinkere R, Suchart S (2023) Agro-waste for renewable and sustainable green production: a review. J Clean Prod 434:139989. https://doi.org/10.1016/j.jclepro.2023.139989

Roldán L, Marco Y, García-Bordejé E (2015) Bio-sourced mesoporous carbon doped with heteroatoms (N, S) synthesised using one-step hydrothermal process for water remediation. Microporous Mesoporous Mater 222:55–62. https://doi.org/10.1016/j.micromeso.2015.10.008

Rong L, Wu L, Zhang T, Hu C, Tang H, Pan H, Zou X (2024) Significant differences in the effects of nitrogen doping on pristine biochar and graphene-like biochar for the adsorption of tetracycline. Molecules 29(1):173. https://doi.org/10.3390/molecules29010173

Ruan G, Yang Y, Peng X, Wang J, Guo Y, Hu W, Lin D (2025) A review of the current status of nitrogen self-doped biochar applications. J Environ Chem Eng 13(1):115291. https://doi.org/10.1016/j.jece.2024.115291

Sajjad M, Sarwar R, Ali T, Khan L, Mahmood SU (2021) Cosmetic uses of activated charcoal. Int J Commun Med Pub Health 8(9):4572–4574. https://doi.org/10.1820/2394-6040.ijcmph20213569

Sami H, Ashraf K, Sultan K, Alamri S, Abbas M, Javied S, Zaman QU (2023) Remediation potential of biochar and selenium for mitigating chromium-induced stress in spinach to minimize human health risk. S Afr J Bot 163:237–249. https://doi.org/10.1016/j.sajb.2023.10.049

Shao Q, Li Y, Wang Q, Niu T, Li S, Shen W (2021) Preparation of copper doped walnut shell-based biochar for efficiently removal of organic dyes from aqueous solutions. J Mol Liq 336:116314. https://doi.org/10.1016/j.molliq.2021.116314

Shen M, Zhu X, Zhang S (2020) Extraneous Fe increased the carbon retention of sludge-based biochar. Bull Environ Contam Toxicol 106(1):198–204. https://doi.org/10.1007/s00128-020-03050-1

Shu R, Zhao Z, Yang X (2023) Fabrication of nitrogen-doped reduced graphene oxide/porous magnesium ferrite@silica dioxide composite with excellent dual-band electromagnetic absorption performance. Chem Eng J 473:145224. https://doi.org/10.1016/j.cej.2023.145224

Siddiqui MN, Redhwi HH, Achilias DS, Kosmidou E, Vakalopoulou E, Ioannidou MD (2017) Green synthesis of silver nanoparticles and study of their antimicrobial properties. J Polym Environ 6(2):423–433. https://doi.org/10.1007/s10924-017-0962-0

Song X, Xing B, Feng J, Yuan J, Ma X, Liu X, Yang G (2020) Degradation of organic dyes by persulfate using liquor grain-derived N, P-codoped

mesoporous carbon as metal-free catalyst. J Water Process Eng 37:101407. https://doi.org/10.1016/j.jwpe.2020.101407
Song J, Li Y, Wang Y, Zhong L, Liu Y, Sun X, He B, Li Y, Cao S (2021) Preparing biochars from cow hair waste produced in a tannery for dye wastewater treatment. Materials 14(7):1690. https://doi.org/10.3390/ma14071690
Song L, Yuan Y, Wang Y, Zhang TC, He G, Yuan S (2024) Cu-MOF-derived Cu nanoparticles decorated porous N-doped biochar for low-temperature H_2S desulfurization. Fuel 368:131682. https://doi.org/10.1016/j.fuel.2024.131682
Sun L, Wang X, Wang Y, Zhang Q (2017) Roles of carbon nanotubes in novel energy storage devices. Carbon 122:462–474. https://doi.org/10.1016/j.carbon.2017.07.006
Sun L, Li L, An X, Qian X (2021) Mechanically strong, liquid-resistant photothermal bioplastic constructed from cellulose and metal-organic framework for light-driven mechanical motion. Molecules 26(15):4449. https://doi.org/10.3390/molecules26154449
Sun C, Du A, Deng G, Zhao X, Pan J, Fu X, Liu J, Cui L, Wang Q (2023a) Naturally nitrogen-doped self-encapsulated biochar materials based on mouldy wheat flour for silicon anode in lithium-ion batteries. Electrochim Acta 450:142269. https://doi.org/10.1016/j.electacta.2023.142269
Sun Y, Jia J, Liu Z, Liu Z, Huo L, Zhao L, Zhao Y, Yao Z (2023b) Heteroatom-doped biochar devised from cellulose for CO_2 adsorption: a new vision on competitive behavior and interactions of N and S. Biochar 5(1):76. https://doi.org/10.1007/s42773-023-00275-1
Sun Z, Liu S, Xu Y, Lu J, Shi H, Li S, Luo C, Dong Q (2023c) Urea impregnation into fungus pretreated corn stover to perform pyrolysis for production of nitrogen-containing bio-oil and nitrogen-doped biochar. Biores Technol 376:128921. https://doi.org/10.1016/j.biortech.2023.128921
Sun Z, Yao D, Guo H, Zhu H, Hua W, Yuan Q, Zhang L, Fan Q, Yi B (2023d) Catalytic mechanism of N-containing biochar on volatile-biochar interaction for the same origin pyrolysis. J Environ Manage 336:117710. https://doi.org/10.1016/j.jenvman.2023.117710
Sun J, Zhang D, Xia D, Li Q (2023e) Orange peels biochar doping with Fe-Cu bimetal for PMS activation on the degradation of bisphenol A: A synergy of SO^{4-}, OH, $^1O_2$ and electron transfer. Chem Eng J 471:144832. https://doi.org/10.1016/j.cej.2023.144832
Sun Y, Jia J, Huo L, Zhao L, Yao Z, Liu Z (2024a) Heteroatom-doped biochar for CO_2 adsorption: a review of heteroatoms, doping methods, and functions. Biomass Convers Biorefinery 14(14):15237–15249. https://doi.org/10.1007/s13399-022-03640-5
Sun A, Bian S, Li L, Guo Z, Li W, Li J, Xu S, Liu PD (2024b) Preparation of highly adsorptive biochar by sequential iron impregnation under refluxing and pyrolysis at low temperature for removal of tetracycline. Environ Pollut 348:123886. https://doi.org/10.1016/j.envpol.2024.123886
Talukdar K, Jun B-M, Yoon Y, Kim Y, Fayyaz A, Park CM (2020) Novel Z-scheme Ag3PO4/Fe3O4-activated biochar photocatalyst with enhanced visible-light catalytic performance toward degradation of bisphenol A. J Hazard Mater 398:123025. https://doi.org/10.1016/j.jhazmat.2020.123025
Tan X, Wei W, Xu C, Meng Y, Bai W, Yang W, Lin A (2020) Manganese-modified biochar for highly efficient sorption of cadmium. Environ Sci Pollut Res 27(9):9126–9134. https://doi.org/10.1007/s11356-019-07059-w
Tang W, Zanli BLGL, Chen J (2021) O/N/P-doped biochar induced to enhance adsorption of sulfonamide with coexisting Cu^{2+}/ Cr (VI) by air pre-oxidation. Biores Technol 341:125794. https://doi.org/10.1016/j.biortech.2021.125794
Tao Y, Sun S, Hu Y, Gong S, Bao S, Li H, Zhang X, Yuan Z, Wu X (2024) Activation of peroxymonosulfate by Fe, O Co-embedded biochar for the degradation of tetracycline: performance and mechanisms. Catalysts 14(9):556. https://doi.org/10.3390/catal14090556
Tian H, Cui K, Sun S, Liu J, Cui M (2023) Sequential doping of exogenous iron and nitrogen to prepare Fe-N structured biochar to enhance the activity of OTC degradation. Sep Purif Technol 322:124249. https://doi.org/10.1016/j.seppur.2023.124249
Verdida RA, Caparanga AR, Chang CT (2023) Facile synthesis of metal-impregnated sugarcane-derived catalytic biochar for ozone removal at ambient temperature. Catalysts 13(2):388. https://doi.org/10.3390/catal13020388
Wan Z, Sun Y, Tsang DCW, Khan E, Yip ACK, Ng YH, Rinklebe J, Ok YS (2020) Customised fabrication of nitrogen-doped biochar for environmental and energy applications. Chem Eng J 401:126136. https://doi.org/10.1016/j.cej.2020.126136
Wan Z, Xu Z, Sun Y, Zhang Q, Hou D, Gao B, Khan E, Graham NJD, Tsang DCW (2022) Stoichiometric carbocatalysis via epoxide-like C–S–O configuration on sulfur-doped biochar for environmental remediation. J Hazard Mater 428:128223. https://doi.org/10.1016/j.jhazmat.2022.128223
Wang J, Wang S (2019) Preparation, modification and environmental application of biochar: a review. J Clean Prod 227:1002–1022. https://doi.org/10.1016/j.jclepro.2019.04.282
Wang B, Wang H, Chen L, Hsueh H, Li X, Guo J, Luo Y, Chiou J, Wang W, Wang P, Chen K, Chen Y, Chen L, Chen C, Wang J, Pong W (2016a) Nonlinear bandgap opening behavior of BN co-doped graphene. Carbon 107:857–864. https://doi.org/10.1016/j.carbon.2016.06.091
Wang L, Jia W, Liu X, Li J, Titirici M (2016b) Sulphur-doped ordered mesoporous carbon with enhanced electrocatalytic activity for the oxygen reduction reaction. J Energy Chem 25(4):566–570. https://doi.org/10.1016/j.jechem.2016.02.012
Wang N, Tong Z, Zhang G, Wang P (2016c) A review on Fenton-like processes for organic wastewater treatment. J Environ Chem Eng 4(1):762–787. https://doi.org/10.1016/j.jece.2015.12.016
Wang L, Wang J, Wang Z, He C, Lyu W, Yan W, Yang L (2018) Enhanced antimonate (Sb(V)) removal from aqueous solution by La-doped magnetic biochars. Chem Eng J 354:623–632. https://doi.org/10.1016/j.cej.2018.08.074
Wang L, Wang J, He C, Lyu W, Zhang W, Yan W, Yang L (2019) Development of rare earth element doped magnetic biochars with enhanced phosphate adsorption performance. Colloids Surfaces A 561:236–243. https://doi.org/10.1016/j.colsurfa.2018.10.082
Wang H, Xu J, Liu X, Sheng L (2020) Preparation of straw activated carbon and its application in wastewater treatment: a review. J Clean Prod 283:124671. https://doi.org/10.1016/j.jclepro.2020.124671
Wang C, Sun R, Huang R (2021a) Highly dispersed iron-doped biochar derived from sawdust for Fenton-like degradation of toxic dyes. J Clean Product 297:126681. https://doi.org/10.1016/j.jclepro.2021.126681
Wang T, Dissanayake PD, Sun M, Tao Z, Han W, An N, Gu Q, Xia D, Tian B, Ok YS, Shang J (2021b) Adsorption and visible-light photocatalytic degradation of organic pollutants by functionalized biochar: role of iodine doping and reactive species. Environ Res 197:111026. https://doi.org/10.1016/j.envres.2021.111026
Wang L-L, Jiang S-F, Huang J, Jiang H (2022) Oxygen-doped biochar for the activation of ferrate for the highly efficient degradation of sulfadiazine with a distinct pathway. J Environ Chem Eng 10(6):108537. https://doi.org/10.1016/j.jece.2022.108537
Wang C, Dai H, Liang L, Li N, Cui X, Yan B, Chen G (2023a) Enhanced mechanism of copper doping in magnetic biochar for peroxymonosulfate activation and sulfamethoxazole degradation. J Hazard Mater 458:132002. https://doi.org/10.1016/j.jhazmat.2023.132002
Wang C, Holm PE, Andersen ML, Thygesen LG, Nielsen UG, Hansen HCB (2023b) Phosphorus doped cyanobacterial biochar catalyzes efficient persulfate oxidation of the antibiotic norfloxacin. Biores Technol 388:129785. https://doi.org/10.1016/j.biortech.2023.129785
Wang X, Huang P, Zhang P, Wang C, Jia H, Sun H (2024) Incorporation of N-doped biochar into submicron zero-valent iron for efficient peroxydisulfate activation in soil remediation: performance and mechanism. Chem Eng J 482:148832. https://doi.org/10.1016/j.cej.2024.148832
Wei W, Pingping W, Chi W, Lan Z, Liangang M, Lizhen Z, Hongyun J, Yongquan Z, Xingang L (2023) Adsorption of acetochlor-contaminated water systems using novel P-doped biochar: Effects, application, and mechanism. Chemosphere 350:141027. https://doi.org/10.1016/j.chemosphere.2023.141027
Wu X, Radovic LR (2006) Inhibition of catalytic oxidation of carbon/carbon composites by phosphorus. Carbon 44(1):141–151. https://doi.org/10.1016/j.carbon.2005.06.038
Wu C, Shi L, Xue S, Li W, Jiang X, Rajendran M, Qian Z (2018) Effect of sulfur-iron modified biochar on the available cadmium and bacterial community structure in contaminated soils. Sci Total Environ 647:1158–1168. https://doi.org/10.1016/j.scitotenv.2018.08.087
Wu J, Wang T, Liu Y, Tang W, Geng S, Chen J (2022) Norfloxacin adsorption and subsequent degradation on ball-milling tailored N-doped biochar. Chemosphere 303:135264. https://doi.org/10.1016/j.chemosphere.2022.135264

Xia C, Surendran S, Ji S, Kim D, Chae Y, Kim J, Je M, Han MK, Choe WS, Choi CH, Choi H, Kim JK, Sim U (2022) A sulfur self-doped multifunctional biochar catalyst for overall water splitting and a supercapacitor from Camellia japonica flowers. Carbon Energy 4(4):491–505. https://doi.org/10.1002/cey2.207

Xiao X, Chen B (2017) A direct observation of the fine aromatic clusters and molecular structures of biochars. Environ Sci Technol 51(10):5473–5482. https://doi.org/10.1021/acs.est.6b06300

Xiao X, Chen B, Zhu L (2014) Transformation, morphology, and dissolution of silicon and carbon in rice straw-derived biochars under different pyrolytic temperatures. Environ Sci Technol 48(6):3411–3419. https://doi.org/10.1021/es405676h

Xin S, Huo S, Zhang C, Ma X, Liu W, Xin Y, Gao M (2021) Coupling nitrogen/oxygen self-doped biomass porous carbon cathode catalyst with $CuFeO_2$/biochar particle catalyst for the heterogeneous visible-light driven photo-electro-Fenton degradation of tetracycline. Appl Catal B 305:121024. https://doi.org/10.1016/j.apcatb.2021.121024

Xu L, Wu C, Liu P, Bai X, Du X, Jin P, Yang L, Jin X, Shi X, Wang Y (2020) Peroxymonosulfate activation by nitrogen-doped biochar from sawdust for the efficient degradation of organic pollutants. Chem Eng J 387:124065. https://doi.org/10.1016/j.cej.2020.124065

Xu Z, Lin Z, Zeng Y, Yang H, Wang Y, Niu M, Xiao Z, Luo J, Lin Z, Chen P, Lv W, Liu G (2025) Preparation of Fe-doped coffee ground biochar and activation of PMS for chloroquine phosphate removal. Appl Surf Sci 679:161160. https://doi.org/10.1016/j.apsusc.2024.161160

Yameen M, Naqvi S, Juchelková D, Khan M (2024) Harnessing the power of functionalized biochar: progress, challenges, and future perspectives in energy, water treatment, and environmental sustainability. Biochar 6(1):25. https://doi.org/10.1007/s42773-024-00316-3

Yan P, Ai F, Cao C, Luo Z (2019) Hierarchically porous carbon derived from wheat straw for high rate lithium ion battery anodes. J Mater Sci: Mater Electron 30(15):14120–14129. https://doi.org/10.1007/s10854-019-01778-z

Yan Z, Huang Z, Zhou H, Yang X, Li S, Zhang W, Wang F, Kuang Y (2020) Facile fabrication of MoP nanodots embedded in porous carbon as excellent anode material for potassium-ion batteries. J Energy Chem 54:571–578. https://doi.org/10.1016/j.jechem.2020.06.037

Yang H, Chen Z, Chen W, Chen Y, Wang X, Chen H (2020) Role of porous structure and active O-containing groups of activated biochar catalyst during biomass catalytic pyrolysis. Energy 210:118646. https://doi.org/10.1016/j.energy.2020.118646

Yang J, Wang J, Li H, Deng Y, Yang C, Zhao Q, Dang Z (2021) Nitrogen-doped biochar as peroxymonosulfate activator to degrade 2,4-dichlorophenol: preparation, properties and structure-activity relationship. J Hazard Mater 424:127743. https://doi.org/10.1016/j.jhazmat.2021.127743

Yang M, Xu C, Dan A, Taiqing W, Zhiping F, Bo W (2022a) Sulfur-doped zero-valent iron supported on biochar for tetracycline adsorption and removal. J Clean Prod 379:134769. https://doi.org/10.1016/j.jclepro.2022.134769

Yang Y, Sun K, Han L, Chen Y, Liu J, Xing B (2022b) Biochar stability and impact on soil organic carbon mineralization depend on biochar processing, aging and soil clay content. Soil Biol Biochem 169:108657. https://doi.org/10.1016/j.soilbio.2022.108657

Yang X, Guo Z, Chen X, Xi S, Cui K, Li J, Dong D, Wu F, Wu Z (2023a) Efficient degradation of thiamethoxam pesticide in water by iron and manganese oxide composite biochar activated persulfate. Chem Eng J 473:145051. https://doi.org/10.1016/j.cej.2023.145051

Yang Y, Zhichao K, Guanghui X, Jian W, Yong Y (2023b) Degradation of bensulfuron methyl by nitrogen/boron codoped biochar activated peroxydisulfate at lower temperature. J Clean Prod 402:136816. https://doi.org/10.1016/j.jclepro.2023.136816

Yang H, Yu Y, Zhang H, Wang W, Zhu J, Chen Y, Zhang S, Chen H (2024a) Effect mechanism of phosphorous-containing additives on carbon structure evolution and biochar stability enhancement. Biochar 6(1):39. https://doi.org/10.1007/s42773-024-00330-5

Yang X, Liu X, Gao H, Zhang C, Chen L, Liao X (2024b) Producing sorbitol from cellulose over Ru-WOX co-doped biochars catalysts. Ind Crops Prod 215:118641. https://doi.org/10.1016/j.indcrop.2024.118641

Yu D, Ma Y, Chen M, Dong X (2018) KOH activation of wax gourd-derived carbon materials with high porosity and heteroatom content for aqueous or all-solid-state supercapacitors. J Colloid Interface Sci 537:569–578. https://doi.org/10.1016/j.jcis.2018.11.070

Yu J, Wu Z, An X, Tian F, Yu B (2021a) Trace metal elements mediated co-pyrolysis of biomass and bentonite for the synthesis of biochar with high stability. Sci Total Environ 774:145611. https://doi.org/10.1016/j.scitotenv.2021.145611

Yu Y, Ren Z, Li L, Han J, Tian Z, Liu C, Chen J (2021b) Ionic liquid-induced graphitization of biochar: N/P dual-doped carbon nanosheets for high-performance lithium/sodium storage. J Mater Sci 56(13):8186–8201. https://doi.org/10.1007/s10853-021-05823-3

Yu J, Tang L, Pang Y, Zhou Y, Feng H, Ren X, Tang J, Wang J, Deng L, Shao B (2022) Non-radical oxidation by N, S, P co-doped biochar for persulfate activation Different roles of exogenous P/S doping, and electron transfer path. J Clean Prod 374:133995. https://doi.org/10.1016/j.jclepro.2022.133995

Yuan C, Chen M, Zhu K, Ni J, Wang S, Cao B, Zhong S, Zhou J, Wang S (2022) Facile synthesis of nitrogen-doped interconnected porous carbons derived from reed and chlorella for high-performance supercapacitors. Fuel Process Technol 238:107466. https://doi.org/10.1016/j.fuproc.2022.107466

Yuan CJ, Song Z-M, Liu M, Chen Y, Ye MQ, Wang WL, Du Y, Wu QY (2023a) Unraveling the evolution of organohalogens and their associated toxicity changes in the chlorination of preozonated reclaimed water containing bromide. ACS ES&T Water 3(11):3570–3580. https://doi.org/10.1021/acsestwater.3c00317

Yuan X, Cao Y, Li J, Patel AK, Dong C-D, Jin X, Gu C, Yip ACK, Tsang DCW, Ok YS (2023b) Recent advancements and challenges in emerging applications of biochar-based catalysts. Biotechnol Adv 67:108181. https://doi.org/10.1016/j.biotechadv.2023.108181

Zaman MW, Phule AD, Elkaee S, Kim SY, Yang JH (2024) Excellent adsorption and catalytic oxidation of toluene facilitated by metal-free nitrogen-doped mesoporous biochar. Sep Purif Technol 353:128378. https://doi.org/10.1016/j.seppur.2024.128378

Zhan W, Zhang X, Yuan Y, Weng Q, Song S, Martínez-López MD, Arauz-Lara JL, Jia F (2024) Regulating chemisorption and electrosorption activity for efficient uptake of rare earth elements in low concentration on oxygen-doped molybdenum disulfide. ACS Nano 18(9):7298–7310. https://doi.org/10.1021/acsnano.4c00691

Zhang K, Min X, Zhang T, Xie M, Si M, Chai L, Shi Y (2021) Selenium and nitrogen co-doped biochar as a new metal-free catalyst for adsorption of phenol and activation of peroxymonosulfate: elucidating the enhanced catalytic performance and stability. J Hazard Mater 413:125294. https://doi.org/10.1016/j.jhazmat.2021.125294

Zhang J, Gu F, Zhou Y, Li Z, Cheng H, Li W, Ji R, Zhang L, Bian Y, Han J, Jiang X, Song Y, Xue J (2022a) Assisting the carbonization of biowaste with potassium formate to fabricate oxygen-doped porous biochar sorbents for removing organic pollutant from aqueous solution. Biores Technol 360:127546. https://doi.org/10.1016/j.biortech.2022.127546

Zhang T, Zhang J, Wei S, Xiong Z, Xiao R, Chuai X, Zhao Y (2022b) Effect of hydrothermal pretreatment on mercury removal performance of modified biochar prepared from corn straw. Fuel 339:126958. https://doi.org/10.1016/j.fuel.2022.126958

Zhang H, Li L, Li Y, He R, Li H, Yu Y (2022c) N and S co-doped pine needle biochar activated peroxydisulfate for antibiotic degradation. J Clean Prod 379:134619. https://doi.org/10.1016/j.jclepro.2022.134619

Zhang H, Xu H, Zi H, Tang Y, Zheng X, Wang P, Huang J, Wu H, Song P, Liu Z, Mao W (2023a) Investigation of the redox behavior of biochar-based bipolar electrochemistry in porous media. Chem Eng J 470:144384. https://doi.org/10.1016/j.cej.2023.144384

Zhang K, Chen Y, Fang Z (2023b) Highly efficient removal of cadmium by sulfur-modified biochar: process and mechanism. Water Air Soil Pollut 234:26. https://doi.org/10.1007/s11270-022-06005-w

Zhao R (2025) A review on the catalytic ozonation of pollutants in wastewater by heteroelements-doped biochar: internal and external doping strategies. Alex Eng J 159:35–44. https://doi.org/10.1016/j.aej.2025.01.088

Zhao S, Li C, Wang W, Zhang H, Gao M, Xiong X, Wang A, Yuan K, Huang Y, Wang F (2013) A novel porous nanocomposite of sulfur/carbon obtained from fish scales for lithium–sulfur batteries. J Mater Chem A 1(10):3334–3339. https://doi.org/10.1039/c3ta01220d

Zhao L, Zheng W, Mašek O, Chen X, Gu B, Sharma BK, Cao X (2017) Roles of phosphoric acid in biochar formation: synchronously improving carbon

retention and sorption capacity. J Environ Qual 46(2):393–401. https://doi.org/10.2134/jeq2016.09.0344
Zhao L, Zhao Y, Nan H, Yang F, Qiu H, Xu X, Cao X (2019) Suppressed formation of polycyclic aromatic hydrocarbons (PAHs) during pyrolytic production of Fe-enriched composite biochar. J Hazard Mater 382:121033. https://doi.org/10.1016/j.jhazmat.2019.121033
Zhao Z, Liu L, Sun Y, Xie L, Liu S, Li M, Yu Q (2023) Combined microbe-plant remediation of cadmium in saline-alkali soil assisted by fungal mycelium-derived biochar. Environ Res 240:117424. https://doi.org/10.1016/j.envres.2023.117424
Zheng X, Wang L, Zhou Y, Luo M, Li H, Bo Z, Zheng W, Chang C, Wen J, Dong J (2023) In-situ synthesis of NiS-modified MgO/S-doped biochar for boosting the adsorption-photocatalytic activity. J Ind Eng Chem 126:492–500. https://doi.org/10.1016/j.jiec.2023.06.037
Zhou Y, Liu X, Xiang Y, Wang P, Zhang J, Zhang F, Wei J, Luo L, Lei M, Tang L (2017) Modification of biochar derived from sawdust and its application in removal of tetracycline and copper from aqueous solution: adsorption mechanism and modelling. Biores Technol 245:266–273. https://doi.org/10.1016/j.biortech.2017.08.178
Zhou C, Liang Y, Xia W, Almatrafi E, Song B, Wang Z, Zeng Y, Yang Y, Shang Y, Wang C, Zeng G (2022a) Single atom Mn anchored on N-doped porous carbon derived from spirulina for catalyzed peroxymonosulfate to degradation of emerging organic pollutants. J Hazard Mater 441:129871. https://doi.org/10.1016/j.jhazmat.2022.129871
Zhou M, Xu Y, Luo G, Zhang Q, Du L, Cui X, Li Z (2022b) Facile synthesis of phosphorus-doped porous biochars for efficient removal of elemental mercury from coal combustion flue gas. Chem Eng J 432:134440. https://doi.org/10.1016/j.cej.2021.134440
Zhou L, Jiang Y, Zhang G, Zhang X, Zhang X, Han L (2023) Pyrolysis-catalysis of medical waste over metal-doping porous biochar to co-harvest jet fuel range hydrocarbons and H2-rich fuel gas. J Anal Appl Pyrol 175:106157. https://doi.org/10.1016/j.jaap.2023.106157
Zhu Y, Liu T, Li L, Song S, Ding R (2017) Nickel-based electrodes as catalysts for hydrogen evolution reaction in alkaline media. Ionics 24(4):1121–1127. https://doi.org/10.1007/s11581-017-2270-z
Zimmerman AR (2010) Abiotic and microbial oxidation of laboratory-produced black carbon (biochar). Environ Sci Technol 44(4):1295–1301. https://doi.org/10.1021/es903140c
Zuo H, Qin X, Liu Z, Fu Y (2021) Preparation and characterization of modified corn stalk biochar. BioResources 16(4):7427–7442. https://doi.org/10.15376/biores.16.4.7428-7443